Bell Telephone Laboratories
Research and Development Unit of the Bell System
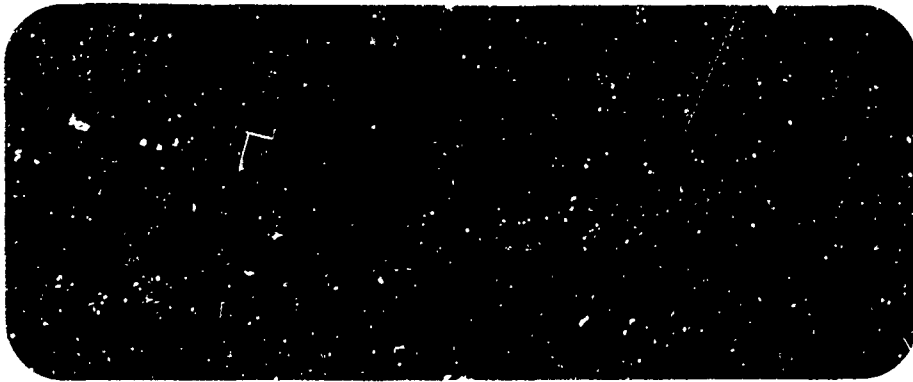
DDC

MAR 27 1968

C
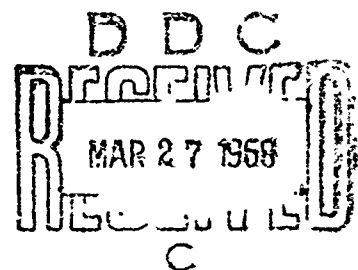
Technical Report No. 14

THE ANALYSIS OF MOORING SYSTEMS
AND RIGID BODY DYNAMICS FOR
SUSPENDED STRUCTURES

December 30, 1966

Distribution of this report is unlimited

ABSTRACT

In this report the response of a moored body to current loadings is investigated. A nonlinear analysis of the steady-state deflections of bipod and tripod moorings is made in Parts I and II. The mooring cables are assumed to be extensible and are loaded with constant gravity and current drag forces. It is shown that the cable weight-in-water is a significant factor in the deflection limited design of a cable system.

In Part III the cable mooring system is represented by linearized equations. Numerical integration is used to investigate the transient rotational and translational response of the moored body to changes in the ambient current.

CONTENTS

Part III

DYNAMICS OF A MOORED RIGID BODY

ILLUSTRATIONS

THE ANALYSIS OF MOORING SYSTEMS AND RIGID BODY DYNAMICS
FOR SUSPENDED STRUCTURES

J. M. Gormally and R. Pringle, December 30, 1966

INTRODUCTION

This report bears on the static and dynamic response of suspended arrays and their mooring systems to varying currents and initial conditions. The results of these considerations play a part in the feasibility studies for different array configurations described in Technical Report No. 13.[1]

Bipod and tripod mooring systems are first examined in some detail. It is shown that a considerable increase in mooring rigidity may be obtained by using neutrally buoyant cable, which reduces the sag in the individual anchor lines. In treating the attitude dynamics of suspended arrays, the structures themselves were assumed perfectly rigid. Numerical calculations are carried out for a tetrahedral and a spherical array showing that these angular excursions due to realistic perturbing forces are indeed quite tolerable.

Part I

DEFLECTION ANALYSIS OF BUOYED BIPOD
AND TRIPOD CABLE SYSTEMS

In this report we present a deflection analysis of buoyed bipod and tripod cable systems. The common cable point is subjected to buoyant lift and current drag forces, and current drag and weight-in-water loadings on each cable are simulated by a distributed loading that has constant magnitude and direction. These loading conditions should provide a realistic measure of the steady-state deflections of the bipod and tripod systems in a deep-ocean operating environment.

---

[1]F. T. Geyling, Technical Report No. _3, "Preliminary Concepts for Suspended Underwater Arrays (U)," Bell Telephone Laboratories for Office of Naval Research, Contract N00014-66-C0005, January 31, 1967, Confidential.

In Section 1 we review the basic solution for an extensible cable deflecting in a plane under a gravity-type loading. Standard cable equations are developed into numerically well conditioned expressions that apply when the total distributed load is small compared with the tension in the cable. This basic solution is extended in Section 2 to treat a single cable in three dimensions subjected to a constant distributed load of arbitrary magnitude and direction.

In Sections 3 and 4 this single cable analysis is employed in a synthesis of the bipod and tripod systems. A Newton-Raphson iteration procedure is proposed for the solution of the fundamental equilibrium and compatibility equations. The cartesian components of the tensions at the common cable point are taken as the fundamental unknowns, and formulas for the trial values are given.

A computer program for the analysis of the tripod system has been generated, and some numerical results are reported in Part II of this report.

1. BASIC CABLE SOLUTION

In this section we review the solution for a single cable under a distributed constant vertical loading. The deflected shape of the cable is referred to a cartesian (X, Y, Z) reference frame (see Figure 1) and the end points on the cable are designated as point 0 and point 1. The relative coordinates [i.e., $(Y_1 - Y_0)$, $(Z_1 - Z_0)$] are expressed in terms of the reactions at point 1, the unstretched length of the cable (L_0), the distributed load (w), and the extensibility of the cable (k). The extended length of the cable is denoted by L.
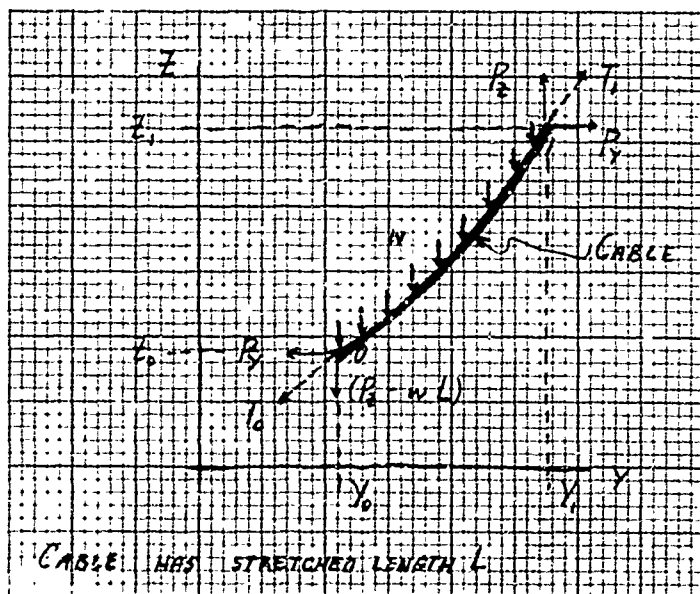
Figure 1. Gravity-Type Loading

2

Defining the tensions T_1 and T_0,

$$T_1 = \left[P_Y^2 + P_Z^2 \right]^{1/2} \tag{1}$$

$$T_0 = \left[P_Y^2 + \left(P_Z - wL \right)^2 \right]^{1/2}, \tag{2}$$

the relative coordinates may be determined from the following expressions:

$$\left(Z_1 - Z_0 \right) = \frac{T_1}{w} \left(1 - \frac{T_0}{T_1} \right) \tag{3}$$

or

$$\left(Z_1 - Z_0 \right) = \left(\frac{L}{T_1} \right) \left(P_Z - \frac{wL}{2} \right) \sum_{k=0}^{\infty} \binom{1/2}{k+1} (-1)^k 2^{k+1} A^k, \tag{4}$$

where

$$A = \left(\frac{wL}{T_1} \right) \frac{P_Z - (wL/2)}{T_1} \tag{5}$$

and

$$\left(Y_1 - Y_0 \right) = \frac{P_Y}{w} \log \left(\frac{T_1 + P_Z}{T_0 + P_Z - wL} \right). \tag{6}$$

or

$$\left(Y_1 - Y_0 \right) = \frac{P_Y \left[L + \left(Z_1 - Z_0 \right) \right]}{T_1 + P_Z} \sum_{k=0}^{\infty} \frac{B^k}{k+1}, \tag{7}$$

where

$$B = \frac{wL \left[1 + \left(Z_1 - Z_0 \right)/L \right]}{T_1 + P_Z}. \tag{8}$$

The series expansions should be used to preserve numerical accuracy when A, B $\leq$ 0.1.

The extended length of the cable is given by

$$L = L_0 + \frac{k}{2} \left[T_0 L + P_Z \left(Z_1 - Z_0 \right) + P_Y \left(Y_1 - Y_0 \right) \right]. \tag{9}$$

3

Remark 1

The equations have been derived under the assumption that the cable is extensible and that w is the distributed load on the cable in its extended (equilibrium) position. They must be solved iteratively to obtain the extended length of the cable.

Remark 2

The modification of these expressions for determining the coordinates of points along the cable is given in the appendix.

To synthesize cable arrays, we require the following partial derivatives that have been developed in compact form:

$$\frac{\partial}{\partial P_Y}\left(Z_1 - Z_0\right) = -\frac{P_Y}{T_0 T_1}\left(Z_1 - Z_0\right), \tag{10}$$

$$\frac{\partial}{\partial P_Z}\left(Z_1 - Z_0\right) = \frac{L}{T_0} - \frac{P_Z\left(Z_1 - Z_0\right)}{T_0 T_1} \tag{11}$$

$$\frac{\partial}{\partial P_Z}\left(Y_1 - Y_0\right) = \frac{\partial}{\partial P_Y}\left(Z_1 - Z_0\right) = -\frac{P_Y}{T_0 T_1}\left(Z_1 - Z_0\right), \tag{12}$$

$$\frac{\partial}{\partial P_Y}\left(Y_1 - Y_0\right) = \frac{\left(Y_1 - Y_0\right)}{P_Y} - \frac{P_Y^2\left(1 - B\right)^{-1}}{T_1\left(T_1 + P_Z\right)}\left[\frac{\left(Z_1 - Z_0\right)}{T_0} + \frac{L + \left(Z_1 - Z_0\right)}{T_1 + P_Z}\right]. \tag{13}$$

In deriving these expressions, we have ignored the extensibility of the cable (i.e., L was treated as a constant). This restriction does not impair the effectiveness of an iteration scheme applied to realistic cable systems because of the smallness of k.

2. SINGLE CABLE — ARBITRARY CONSTANT LOADING

In this section we consider the deflections of a single cable in three dimensions subjected to a constant distributed loading of arbitrary magnitude and direction (Figure 2). With these loading conditions, the cable will deflect in a plane determined by the distributed loading vector and the cable tensions. In this plane, the basic cable expressions of the previous section apply (after an appropriate rotation of the coordinate system).

4
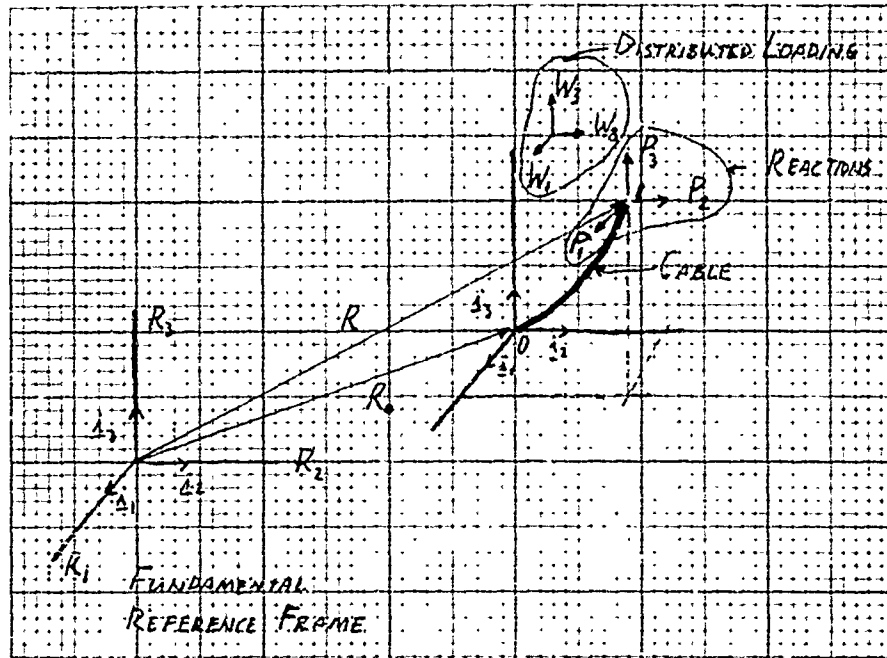
Figure 2. Cable In Three Dimensions

Remark 3

We employ upper case letters to denote vectors, and subscripts 1, 2, 3 to denote their cartesian components in the fundamental frame (Figure 2).

We proceed by introducing a set of unit vectors I, J, K. The K vector is selected so that it is in a direction opposite to the total distributed load $W = (W_1, W_2, W_3)$.

$$K = \left(K_1, K_2, K_3\right) = \left(-\frac{W_1}{|W|}, -\frac{W_2}{|W|}, -\frac{W_3}{|W|}\right) \tag{14}$$

$$|W| = \left(W_1^2 + W_2^2 + W_3^2\right)^{1/2}. \tag{15}$$

The unit normal to the plane defined by W and the cable tension at point 1
$[P = (P_1, P_2, P_3)]$ is given by

$$I = \left(I_1, I_2, I_3\right) = \frac{P \times K}{|P \times K|}. \tag{16}$$

The triad is completed by defining

$$J = \left(J_1, J_2, J_3\right) = K \times I \tag{17}$$

$$= \frac{K \times (P \times K)}{|P \times K|} = \frac{P - K(K \cdot P)}{|P \times K|}.$$

5

The cartesian components of the cable point 1 $[R = (R_1, R_2, R_3)]$ are given in the fundamental reference frame (Figure 2) by

$$R_i = R_{0i} + J_i \left(Y_1 - Y_0\right) + K_i\left(Z_1 - Z_0\right) \quad (i = 1,2,3). \tag{18}$$

Since the cartesian components of the vector P may, in the fundamental frame, be written as

$$P_i = P_Y J_i + P_Z K_i \quad (i = 1,2,3), \tag{19}$$

we have

$$P_Y = \sum_{i=1}^{3} P_i J_i, \quad P_Z = \sum_{i=1}^{3} P_i K_i. \tag{20}$$

To synthesize a cable network, we require the sensitivities of R to changes in the reaction P. These quantities may be calculated from the following set of expressions (i, j = 1,2,3).

$$\frac{\partial R_i}{\partial P_j} = \frac{\partial J_i}{\partial P_j} \left(Y_1 - Y_0\right) + J_1 \left\{ \left[\frac{\partial}{\partial P_Y}\left(Y_1 - Y_0\right) + \frac{\partial}{\partial P_Y}\left(Z_1 - Z_0\right)\right]\frac{\partial P_Y}{\partial P_j} \right.$$
$$\left. + \left[\frac{\partial}{\partial P_Z}\left(Y_1 - Y_0\right) + \frac{\partial}{\partial P_Z}\left(Z_1 - Z_0\right)\right]\frac{\partial P_Z}{\partial P_j} \right\}, \tag{21}$$

where

$$\frac{\partial P_Z}{\partial P_j} = K_j \qquad \frac{\partial P_Y}{\partial P_j} = J_j + \sum_{i=1}^{3} P_i \frac{\partial J_i}{\partial P_j} \tag{22}$$

$$\frac{\partial J_i}{\partial P_j} = \left[\left(\frac{\partial P_i}{\partial P_j} - K_i K_j\right)\frac{J_i}{|P \times K|}\frac{\partial}{\partial P_j}|P \times K|\right]|P \times K|^{-1}. \tag{23}$$

The partial derivatives of the scalar $|P \times K|$ are given by

$$|P \times K| \frac{\partial}{\partial P_1}|P \times K| = -K_3\left(P_3 K_1 - P_1 K_3\right) + K_2\left(P_1 K_2 - P_2 K_1\right),$$

$$|P \times K| \frac{\partial}{\partial P_2}|P \times K| = +K_3\left(P_2 K_3 - P_3 K_2\right) + K_1\left(P_1 K_2 - P_2 K_1\right). \tag{24}$$

$$|P \times K| \frac{\partial}{\partial P_3}|P \times K| = -K_2\left(P_2 K_3 - P_3 K_2\right) + K_1\left(P_3 K_1 - P_1 K_3\right).$$

Remark 4

The complexity of the expressions (21) to (24) is of course caused by the dependence of the vectors I and J upon the reaction P.

6
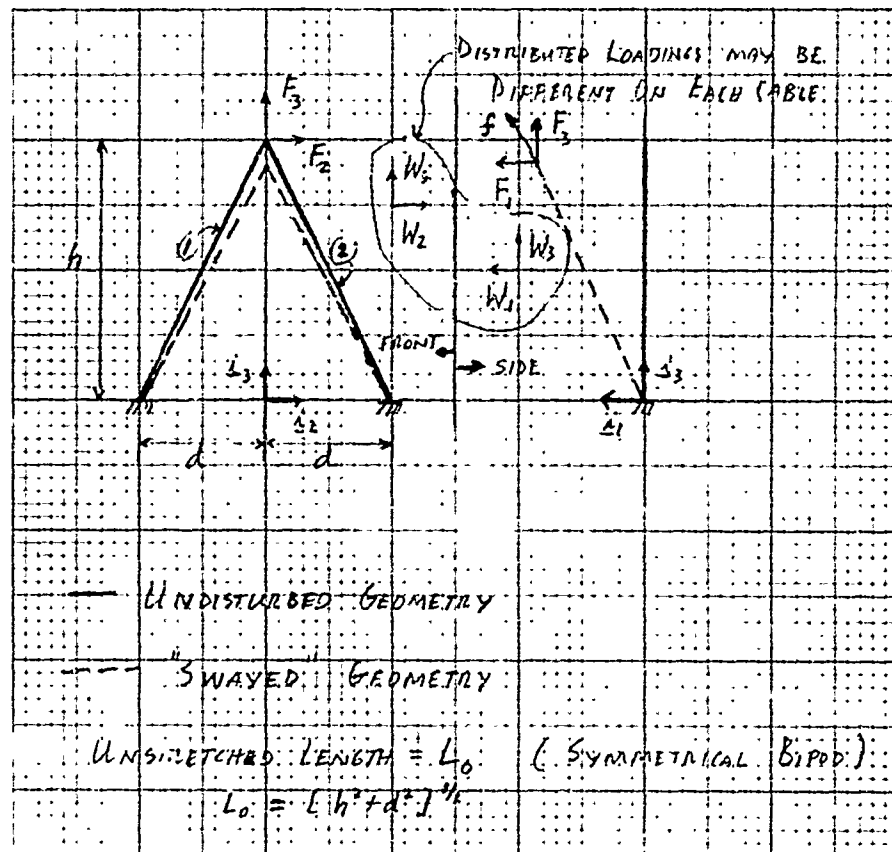
Figure 3. Bipod System

Remark 5

The quantities $(Y_1 - Y_0)$ and $(Z_1 - Z_0)$ are calculated by the expressions in Section 1. The quantities P_Y and P_Z are provided by (20) and $w = |W|$. The unstretched length of cable L_0 and the extensibility of the cable are assumed known.

In the following section, we apply the results developed in the present section to the analysis of the bipod system.

3. APPLICATION TO THE BIPOD SYSTEM

The bipod cable system is illustrated in Figure 3, where the fundamental reference frame with unit vectors $(\underline{i}_1, \underline{i}_2, \underline{i}_3)$ is defined. Each cable in the system is subjected to a constant distributed loading, and the buoyed joint is subjected to a loading $F = (F_1, F_2, F_3)$, which results from buoyant lift and current drag.

7

Let us adopt a sign convention for the forces based on the unit vectors $(\underline{i}_1, \underline{i}_2, \underline{i}_3)$ and designate the cable reactions at the tops of cables 1 and 2 by $P^1 = \left(P_i^1\right)$, $P^2 = \left(P_i^2\right)$, respectively. The equations of equilibrium of the buoyed joint may then be written as

$$C_i = F_i - P_i^1 - P_i^2 = 0 \quad (i = 1,2,3). \tag{25}$$

The conditions for compatible displacement of the buoyed joint require that

$$C_{i+3} = R_i^1 - R_i^2 = 0 \quad (i = 1,2,3) \tag{26}$$

where $R^1 = \left(R_i^1\right)$ and $R^2 = \left(R_i^2\right)$ determine the joint position as calculated along cables 1 and 2, respectively, from the origin of the fundamental reference frame.

Equations (25) and (26) provide six equations for the six unknowns $P^1 = \left(P_i^1\right)$, $P^2 = \left(P_i^2\right)$, $(i = 1,2,3)$. We propose that these six equations be solved iteratively by a Newton-Raphson procedure. Trial values of the quantities P^1, P^2 are given at the end of this section.

The Newton-Raphson method requires the partial derivatives of the equations of condition C_k ($k = 1, \ldots, 6$) with respect to the unknowns $\left(P_i^1\right)$, $\left(P_i^2\right)$, $(i = 1,2,3)$. The required array may be written in the form

$$\begin{bmatrix} \dfrac{\partial C_k}{\partial P_i^1}, & \dfrac{\partial C_k}{\partial P_i^2} \end{bmatrix} \qquad \begin{array}{l} (k = 1, \ldots, 6) \\ (i = 1,2,3) \end{array}. \tag{27}$$

Taking the partial derivatives of (25) and (26) we have the results*

$$\frac{\partial C_i}{\partial P_j^1} = \frac{\partial C_i}{\partial P_j^2} = -\delta_{ij} \qquad (i,j = 1,2,3), \tag{28}$$

$$\frac{\partial C_{i+3}}{\partial P_j^1} = \frac{\partial R_i^1}{\partial P_j^1}, \qquad \frac{\partial C_{i+3}}{\partial P_j^2} = -\frac{\partial R_i^2}{\partial P_j^2} \quad (i,j = 1,2,3) \tag{29}$$

The partial derivatives in (29) are provided by the expressions in Section 2.

In determining trial values for the cable reactions, it is convenient to ignore the distributed loadings and base the estimates on the load F and the "swayed" geometry of the bipod. Let us define E^1, E^2 as the unit vectors along the legs of the "swayed" bipod. The equilibrium of the buoyed joint gives

$$F_i - \left(|P^1| E_i^1 + |P^2| E_i^2\right) = 0 \quad (i = 1,2,3). \tag{30}$$

$*\delta_{ij} = 1 \quad (i = j)$
$\phantom{*\delta_{ij}} = 0 \quad (i \neq j)$

8

If we solve these equations for $|P^1|$ and $|P^2|$, the trial values are given by $P_i^1 = |P^1|E_i^1,\ldots,$. The "swayed" geometry is defined by the unit vectors

$$E^1 = \left(\frac{F_1}{f}, \frac{d}{L_0}, \frac{F_3}{f}\right)$$

$$E^2 = \left(\frac{F_1}{f}, \frac{-d}{L_0}, \frac{F_3}{f}\right)$$

(31)

where

$$f = \left(F_1^2 + F_3^2\right)^{1/2}.$$

(32)

Solving (3), we obtain

$$|P^1| = \frac{1}{2}\left(f + \frac{dF_2}{L_0}\right),$$

$$|P^2| = \frac{1}{2}\left(f - \frac{dF_2}{L_0}\right).$$

(33)

4. APPLICATION TO THE TRIPOD SYSTEM

The analysis of the tripod system (Figure 4) parallels that of the bipod system in the previous section. The unknowns are the cartesian components of the cable reactions P^1, P^2, P^3, and the equilibrium of the buoyed joint is specified by the equations

$$C_i = F_i - P_i^1 - P_i^2 - P_i^3 \quad (i = 1,2,3).$$

(34)

The conditions for the compatible displacement of the buoyed joint require that

$$C_{i+3} = R_i^1 - R_i^2 = 0$$

$$C_{i+6} = R_j^1 - R_i^3 = 0$$

$$(i = 1,2,3),$$

(35)

where $\left(R_i^1\right)$, $\left(R_i^2\right)$, and $\left(R_i^3\right)$ determine the joint position as calculated along cables 1, 2, and 3, respectively, from the origin of the fundamental reference frame.

The array of partial derivatives of the equations of condition (34) and (35) may be written in the form
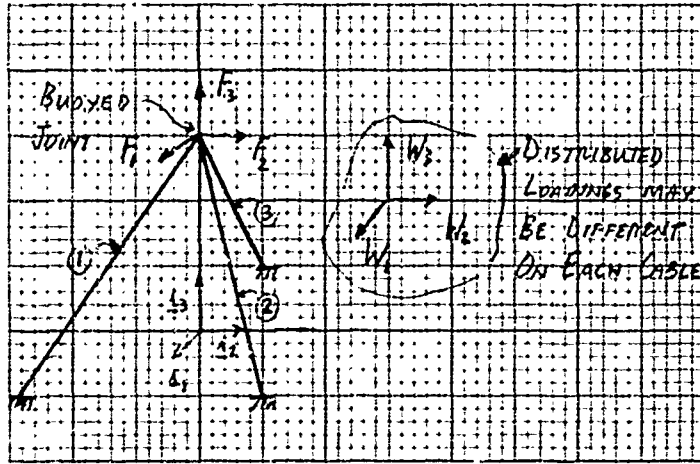
9

Figure 4. Tripod System

$$\begin{bmatrix} \dfrac{\partial C_k}{\partial P_j^1}, & \dfrac{\partial C_k}{\partial P_j^2}, & \dfrac{\partial C_k}{\partial P_j^3} \end{bmatrix} \qquad \begin{matrix} (k = 1, \dots, 9) \\ (j = 1,2,3) \end{matrix}. \tag{36}$$

Taking the various partial derivatives of (34) and (35), we obtain

$$\frac{\partial C_i}{\partial P_j^1} = \frac{\partial C_i}{\partial P_j^2} = \frac{\partial C_i}{\partial P_j^3} = -\delta_{ij} \qquad (i,j = 1,2,3), \tag{37}$$

$$\frac{\partial C_{i+3}}{\partial P_j^1} = \frac{\partial R_i^1}{\partial P_j^1}, \ \frac{\partial C_{i+3}}{\partial P_j^2} = -\frac{\partial R_i^2}{\partial P_j^2}, \ \frac{\partial C_{i+3}}{\partial P_j^3} = 0, \tag{38}$$

$$\frac{\partial C_{i+6}}{\partial P_j^1} = \frac{\partial R_i^1}{\partial P_j^1}, \ \frac{\partial C_{i+6}}{\partial P_j^2} = 0, \ \frac{\partial C_{i+6}}{\partial P_j^3} = -\frac{\partial R_i^3}{\partial P_j^3} \ (i,j = 1,2,3). \tag{39}$$

As before, the partial derivaties in (38) and (39) are provided by the expressions in Section 2.

In determining trial values for the reactions, it is convenient to ignore the distributed loading and base the estimates upon the load F and the initial geometry of the tripod. Let us define E^1, E^2, E^3 as the unit vectors along the legs of the tripod (undisturbed position). The equilibrium of the buoyed joint gives

$$F_i - \left(|P^1| E_i^1 + |P^2| E_i^2 + |P^3| E_i^3 \right) = 0 \quad (i = 1,2,3). \tag{40}$$

10

If we solve these equations for the quantities $|P^1|$, $|P^2|$, $|P^3|$, the trial values are give by $P_i^1 = |P^1| E_i^1$, etc. For cable structures under consideration, the members, of course, must always be in tension.
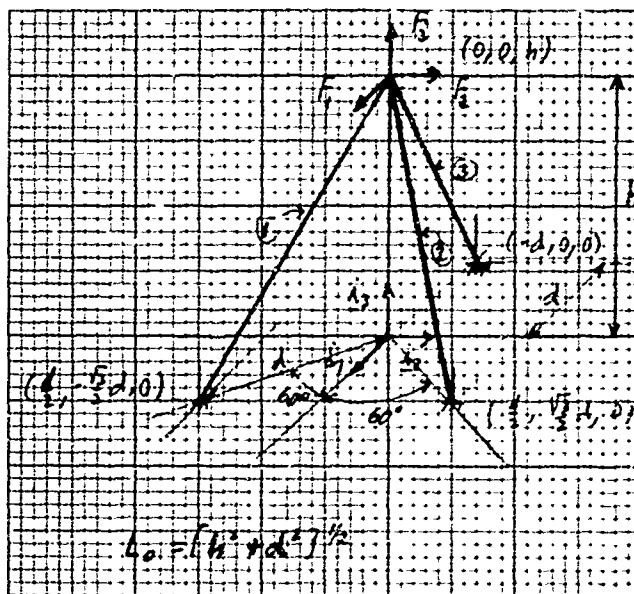

Figure 5. Symmetrical Tripod

For the case of the symmetrical tripod pictured in Figure 5, the unit vectors are given by

$$E^1 = \left(\frac{-d}{2L_0}, \frac{\sqrt{3}d}{2L_0}, \frac{h}{L_0} \right),$$

$$E^2 = \left(\frac{-d}{2L_0}, \frac{-\sqrt{3}d}{2L_0}, \frac{h}{L_0} \right), \qquad (41)$$

$$E^3 = \left(\frac{d}{L_0}, 0, \frac{h}{L_0} \right)$$

11

Using these values, we obtain

$$|P^1| = \frac{L_0}{3d}\left(\frac{d}{h}\,F_3 + \sqrt{3}\,F_2 - F_1\right),$$

$$|P^2| = \frac{L_0}{3d}\left(\frac{d}{h}\,F_3 - \sqrt{3}\,F_2 - F_1\right), \tag{42}$$

$$|P^3| = \left(\frac{L_0}{3h}\,F_3 + \frac{2}{3}\frac{L}{d}\,F_1\right).$$

5. CURRENT LOADING ON THE CABLES

In this section we present the expressions for calculating the current loading on the cables. We assume that the basic theory for flow around rough cylinders applies to the cables and that we may use the associated normal and tangential drag coefficients.

Let us define E as the unit vector along the undisturbed direction of the cable. We assume that the current forces act in a plane defined by this vector and the stream velocity vector $V = (V_1, V_2, V_3)$. We define a unit vector normal to the cable and contained in this plane by the expression

$$N = \frac{E \times (V \times E)}{|V \times E|} = \frac{V - E(V \cdot E)}{|V \times E|}. \tag{43}$$

The components of velocity in the normal and tangential directions are given by

$$V_T = V \cdot E,$$

$$V_N = V \cdot N. \tag{44}$$

Using the standard drag expressions, the normal and tangential forces per unit length are determined as

$$F_N \quad \frac{1}{2}\,C_{DN}\,\rho d_c \left(V_N\right)^2, \tag{45}$$

and

$$F_T = \frac{1}{2}\,C_{DT}\,\rho d_c \left(V_T\right)^2, \tag{46}$$

where C_{DN} and C_{DT} are the normal and tangential drag coefficients, respectively. The cable diameter is denoted by d_c, and ρ is the density of water.

The cartesian components of the current loading are given by

$$F_T E_i + F_N N_i \qquad (i = 1,2,3). \tag{47}$$

12

6. SUMMARY

We have presented the fundamental equations for determining the steady-state deflections of current loaded bipod and tripod cable systems. These equations were developed under the assumption that the distributed current loading on the individual cables could be approximated by distributed loading with constant magnitude and direction. Numerical experience with a practical tripod system showed that the cable slope varies by less than 0.5 percent (even with large buoy drag loads), so that this assumption is extremely good. Some material related to the present problem may be found in other documents.[2,3]

---

[2] Basil W. Wilson, "Characteristics of Anchor Cables in Uniform Ocean Currents," Texas A&M Research Foundation Report No. 204-1, April 1960.

[3] W. T. O'Brien and A. J. Francis, "Cable Movements Under Two-Dimensional Loads," J. Struc. Div. ASCE, June 1963, pp 89-123.

Appendix

COORDINATES OF POINTS ALONG A SINGLE CABLE

The coordinates of points along a single cable may be obtained by a simple modification of the equations in Section 1.

To find the stretched coordinates of a point S^* on the unstretched cable, we first solve (1) through (9) to obtain L. Then we employ the same equations, substituting $[P_Z - W(L - S)]$ for P_Z, and S, and S^* for L and L_0, respectively. The quantity S clearly stands for the stretched location along the cable of the point S^*. Equations (1) through (9), with the stated substitution, now yield $[Y(S^*) - Y_0]$ and $[Z(S^*) - Z_0]$.

Part II

DEFLECTIONS OF BUOYED TRIPOD CABLE SYSTEMS
UNDER CURRENT LOADING

We present here some numerical results for the steady-state deflections of a buoyed symmetrical tripod structure under current loading expected in a deep ocean environment. The primary object of this study is to identify the most significant factors in the deflection-limited design of buoyed tripod cable systems. As such, the study is not intended to be a parametric investigation sufficient for the optimum design of these structures.

The numerical results were generated by the SPIDER program on the GE DSCS (Desk Side Computer System). This program employs the analysis given in Part I of this report.

In Section 1 we review the symmetrical tripod geometry and delineate the cable and loading parameters under consideration. In Section 2 we examine the preliminary design of the cables and present data on the buoyant lift and current drag forces on lithium-filled buoys. We also establish limits on the geometry of the tripod and consider the design of neutrally buoyant cables.

The influence of the loading and cable parameters on the tripod deflections is explored in Section 3. The cable weight-in-water was found to have a most significant influence on the tripod deflections. The stiffness of the tripod increases substantially with a reduction of the cable weight-in-water (for fixed cable strength). Certain generalizations relating to tripod deflection response are made in Section 4 and extensions of the present investigation are recommended.

1. BUOYED TRIPOD STRUCTURE AND LOADINGS

The geometry of a symmetrical tripod cable system is illustrated in Figure 6. The base projections of the cable legs are separated by 120 degrees and the fundamental bent geometry is specified by a height parameter h and a base parameter d. The cables are defined by their diameters d_c, unit weight-in-water w_c, extensibility k_c, and unstretched length L_0.
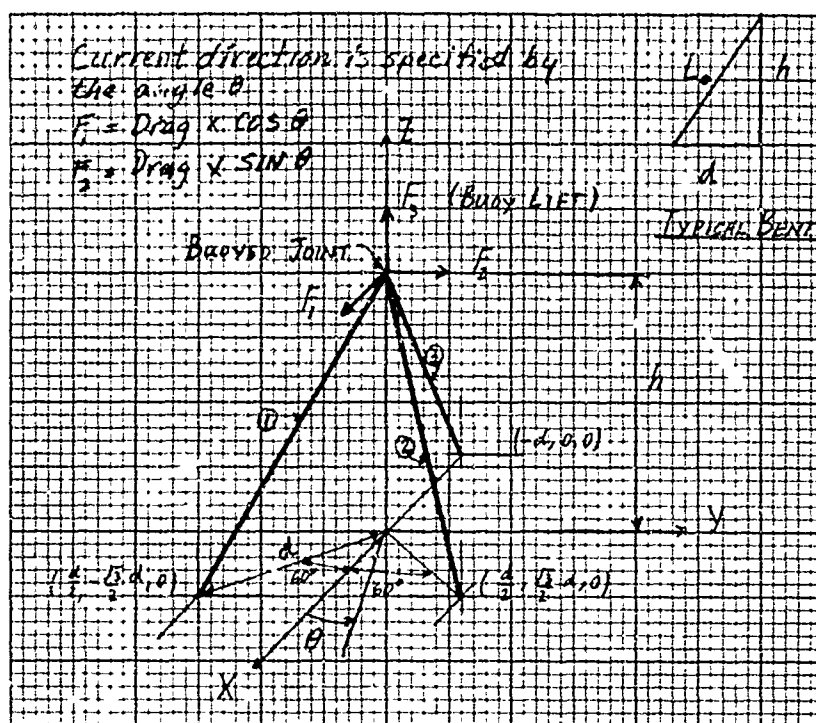
15

Figure 6. Symmetrical Tripod

The loading on the tripod is defined by buoyant lift and drag forces on the buoyed joint and the current drag and weight-in-water loadings on the cable. The range of buoy drag forces considered is an order of magnitude larger than the normal buoy drag resulting from flow around a sphere. This extended range allows us to examine deflections when a large structure is appended to the buoy, or when two tripods are used as anchors for a structure with connections at the buoyed joint.

Because we are interested in situations where the deflections are small compared with the height parameter h, the current loadings on the cables are calculated on the basis of the initial cable geometry. These forces are assumed to act in a plane defined by the current velocity vector and the initial cable axis, and are resolved into normal and tangential components according to the usual theory of flow around rough cylinders.[4] The expressions used in the SPIDER program are given in Section 5 of Part I of this report. In the following section we consider the preliminary design of the cables in the tripod structure.

---

[4]Wilson, op. cit.

2. PRELIMINARY DESIGN

In the present version of the SPIDER program, cable sizing is performed on the basis of initial tripod geometry and buoy lift force, using a factor of safety (FS) of 3. This procedure has proved extremely useful, since the maximum cable tension changes very little with the addition of buoy drag, cable weight, and current loading.

In Figure 7 we have plotted the variation in maximum cable tension (solid line) due to the addition of buoy drag for various fixed-lift forces. The initial design tension is shown as the dashed line. We observe that the additional cable weight relieves tension in the cables (this is accomplished by the increased cable slope at the buoy).
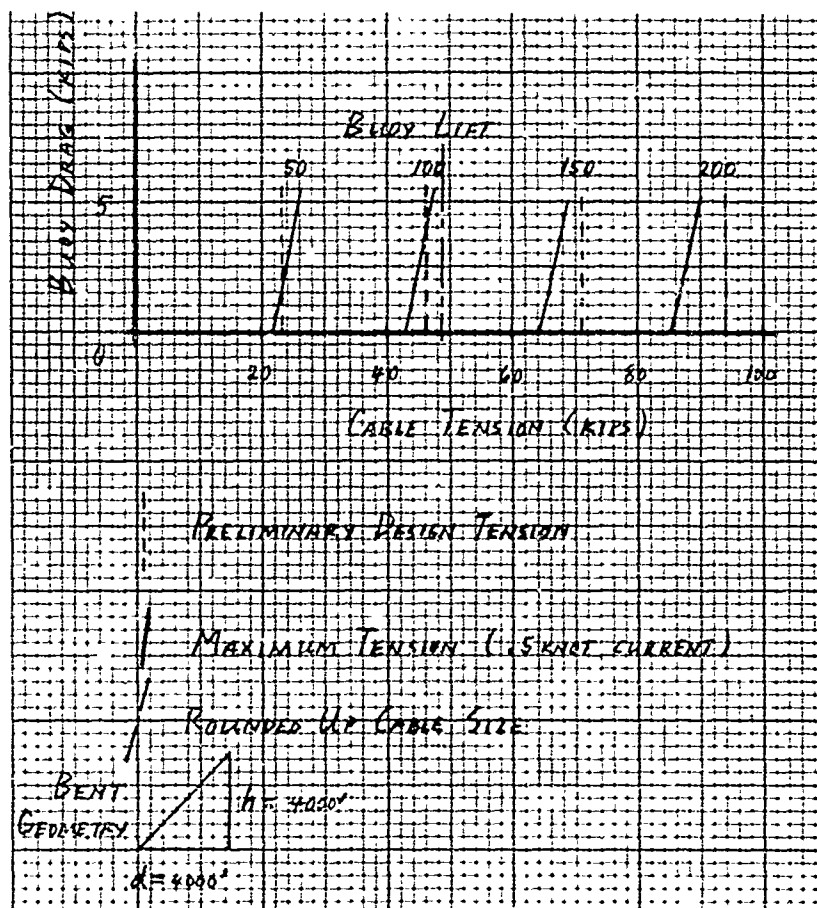

Figure 7. Cable Tension Variations

17

The initial cable size is selected on the basis of an empirical expression relating ultimate cable strength T_u to cable diameter d_c. This expression,

$$T_u = 70 \ d_c^2 \ \text{kips} \tag{1}$$

$$(d_c \ \text{in inches}),$$

was obtained from Wilson[5] and checked against the data for 6 x 24 steel mooring line in Baumeister[6]. Cable weight-in-water for these cables is given by Wilson[7].

$$w_c = 1.25 \ d_c^2 \ \text{lb/ft}. \tag{2}$$

The extensibility* (as defined in Part I) of these cables was estimated on the basis of steel cross-sectional area by

$$k_c = \frac{6.67 \times 10^{-5}}{d_c^2}. \tag{3}$$

Considering only the buoy lift force F_3, the preliminary cable sizing for the symmetrical tripod was performed using the following expression

$$d_c = \left[\left(\frac{L_0}{h} \right) \frac{F_3 (FS)}{210} \right]^{1/2} \tag{4}$$

where F_3 is given in kips. Actual cables were selected by rounding off this number to the nearest cable size.

The expressions (1) through (4) are displayed graphically in Figure 8. For a given lift force and factor of safety of cable design, we may obtain the preliminary cable diameter and weight for various values of the ratio h/d.

2.1 Possible Bent Configurations

The bent configuration of a symmetrical tripod is specified by the height parameter h and the base parameter d. The expressions (1) through (4) may be employed to show that for fixed h, d, the ratio K of buoy lift to total cable weight remains a constant. Conversely, for fixed K the quantities h and d must take restricted values.

---

[5]Wilson, op. cit. p. 47.

[6]T. Baumeister, Ed. Mark's Mechanical Engineering Handbook. New York McGraw-Hill Book Co., 1958.

[7]Wilson, op cit., p. 41.

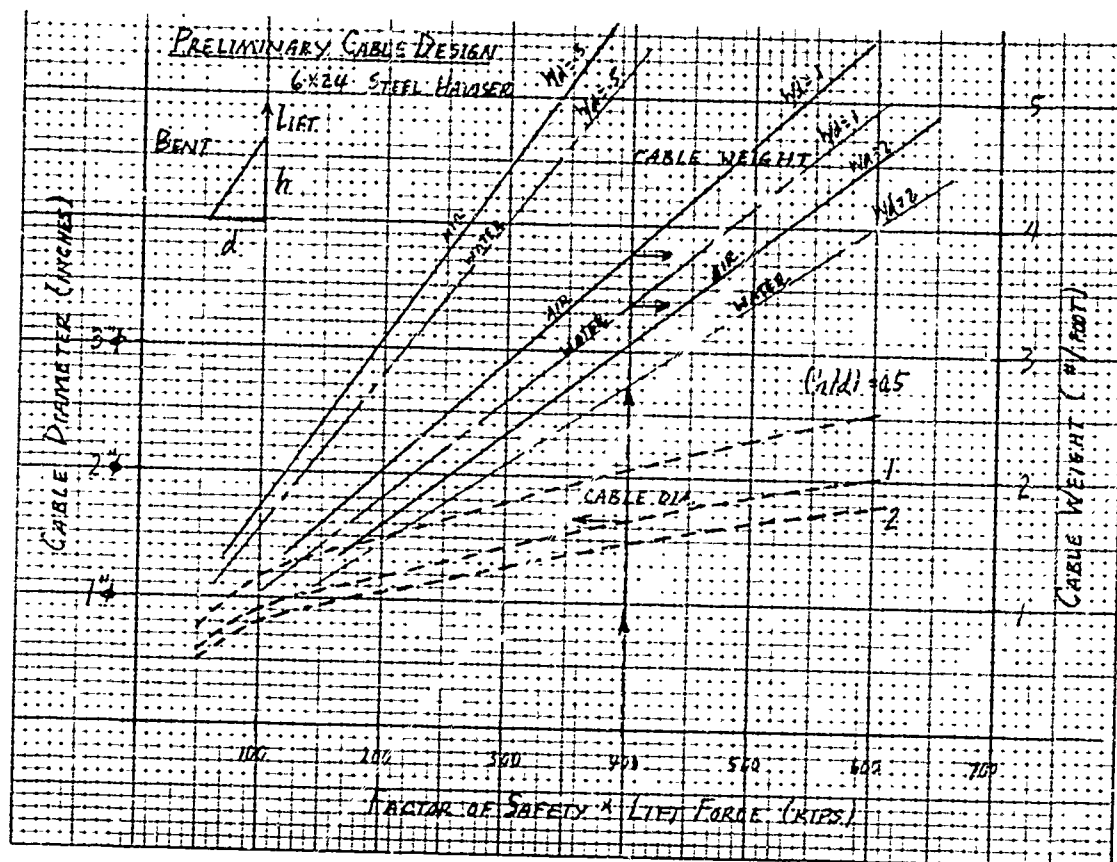*The extensibility (k_c) is the extension in feet over a one-foot length of cable per kip of applied load.

Figure 8. Preliminary Cable Design

To avoid collapse of the structure, we require K > 1 and this condition defines the class of possible bent configurations. This criterion may be developed in the form

$$\frac{h}{d} > \left(\frac{xh}{1 - xh}\right)^{1/2} \quad \text{(h in feet)},\tag{5}$$

where

$$x = 1.79 \times 10^{-5} \, (FS) \, (K) \, (B)$$
$$= 1.79 \times 10^{-5} \, \eta.$$

In developing (5) we have allowed for the variation in FS and incorporated the parameter B = (floated cable weight/cable weight-in-water) to allow for cable weight reduction by the use of floats. In this formulation the quantity η is a constant for a given geometry h, d.

19

The inequality (5) is displayed graphically in Figure 9 where h/d is plotted as a function of h for various values of $\eta = (FS) (K) (B)$.

Example 1. Taking FS = 3 and B = 1, the possible bent configurations lie above the $\eta = 3$ curve in Figure 9. If h = 8000 feet, the base d must be less than 8900 feet.
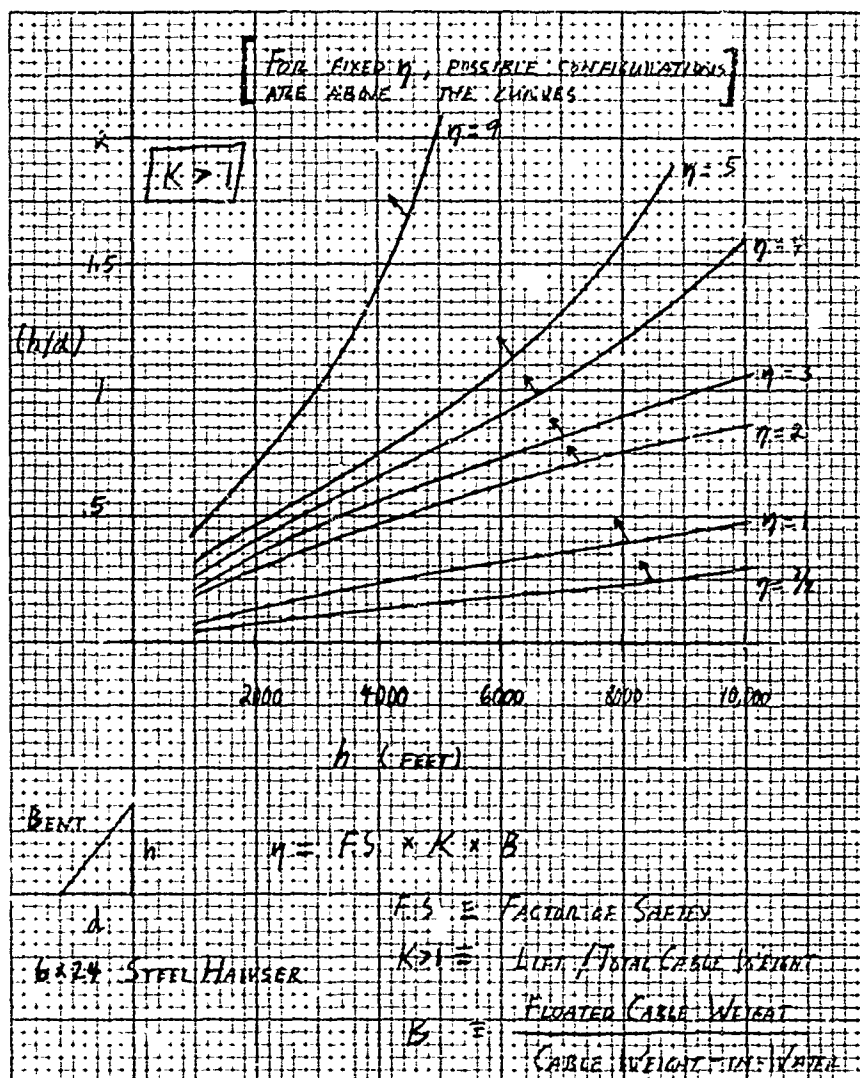

Figure 9. Possible Bent Configurations

20

2.2 Buoy Design

Very efficient buoy designs for deep ocean operations may be obtained through the use of gasoline or lithium-filled spheres. As an example for which there is some experience, we will confine our attention to lithium-filled spherical shells (wall thickness 1/4 inch) used in the Project Trident vertical array at Bermuda.[8]

The lift and drag forces on these buoys may be approximated by the expressions

$$\text{Lift} = 12 \left(\frac{d_b}{10} \right)^{3.26} \text{ (kips)} \tag{6}$$

$$\text{Drag} = 8.6 \times 10^{-4} \, V^2 \, d_b^{\,2} \text{ (kips)} \tag{7}$$

where V is the current velocity in knots and d_b is the buoy diameter in feet.

To obtain a given lift force by the use of N buoys, the buoy diameter can be selected by the expression

$$d_b = 4.67 \left(\frac{\text{Lift}}{N} \right)^{0.307} \text{ (feet)} \tag{8}$$

Example 2. A lift of 100 kips may be obtained by using one buoy at 19.2 feet, two buoys at 15.6 feet, or three buoys at 13.7 feet each. The respective drag forces in a 1 knot current are 0.32, 0.42, and 0.48 kips.

The expressions (6) - (8) are displayed graphically in Figure 10. As indicated previously, we consider a range of drag forces an order of magnitude larger than those resulting from flow around a sphere (up to 10 kips).

2.3 Neutrally Buoyant Cables

In our numerical investigation we observed that cable weight was a significant factor in the deflection response of the tripod. In this subsection we consider the design of cylindrical floats concentric with the cable and spaced to provide an almost neutrally buoyant cable.

If we consider floats with density ρ_f and length L_1, and use the expression $1.4 \, d_c^2$ lb/ft (d_c in inches) for the cable weight-in-air, the following nondimensional expression can be readily derived

$$\frac{d_f}{d_c} = \left(\frac{4\lambda - \kappa}{1 - \kappa} \right)^{1/2}, \tag{9}$$

---

[8]H. M. Kruchten, Determination of the Drag-to-Lift Ratio for Spherical Buoys at Depths to 15,000 Feet, Bell Telephone Laboratories unpublished work.
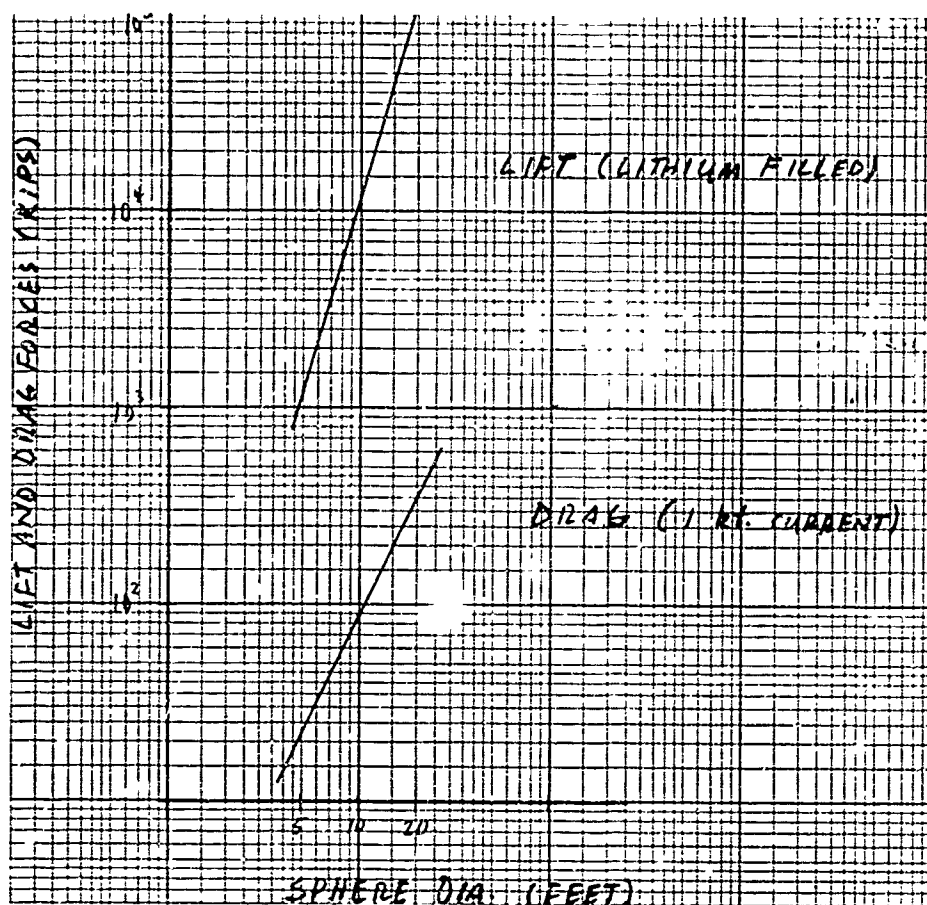
21

Figure 10. Lift and Drag Forces on Lithium-Filled Spheres

where d_f is the outer float diameter, $\lambda = L_2/L_1$, L_2 is the float spacing, and $\kappa = \rho_f/\rho_w$ where ρ_w is the density of water ≈ 64 lb/ft^3.

The relation (9) is displayed in Figure 11 where d_f/d_c is plotted as a function of $\kappa = \rho_f/\rho_w$ for various values of the spacing-size parameter.

Example 3. For float material such as an epoxy-glass matrix[9] $\rho f \approx 45$ lb/ft^3, $\kappa \approx 0.7$, a continuous coat ($\lambda = 1$) would have an outside diameter of ≈ 2-1/2 inches for a 1 inch cable. The use of 1 foot long floats at a spacing of 10 feet would require an outside diameter of 9 inches for a 1 inch cable.

---

[9]Interim Report on Properties of Buoyant Materials and Structures, Proteus, Inc., Contract NONR-4271(00), May 8, 1964.
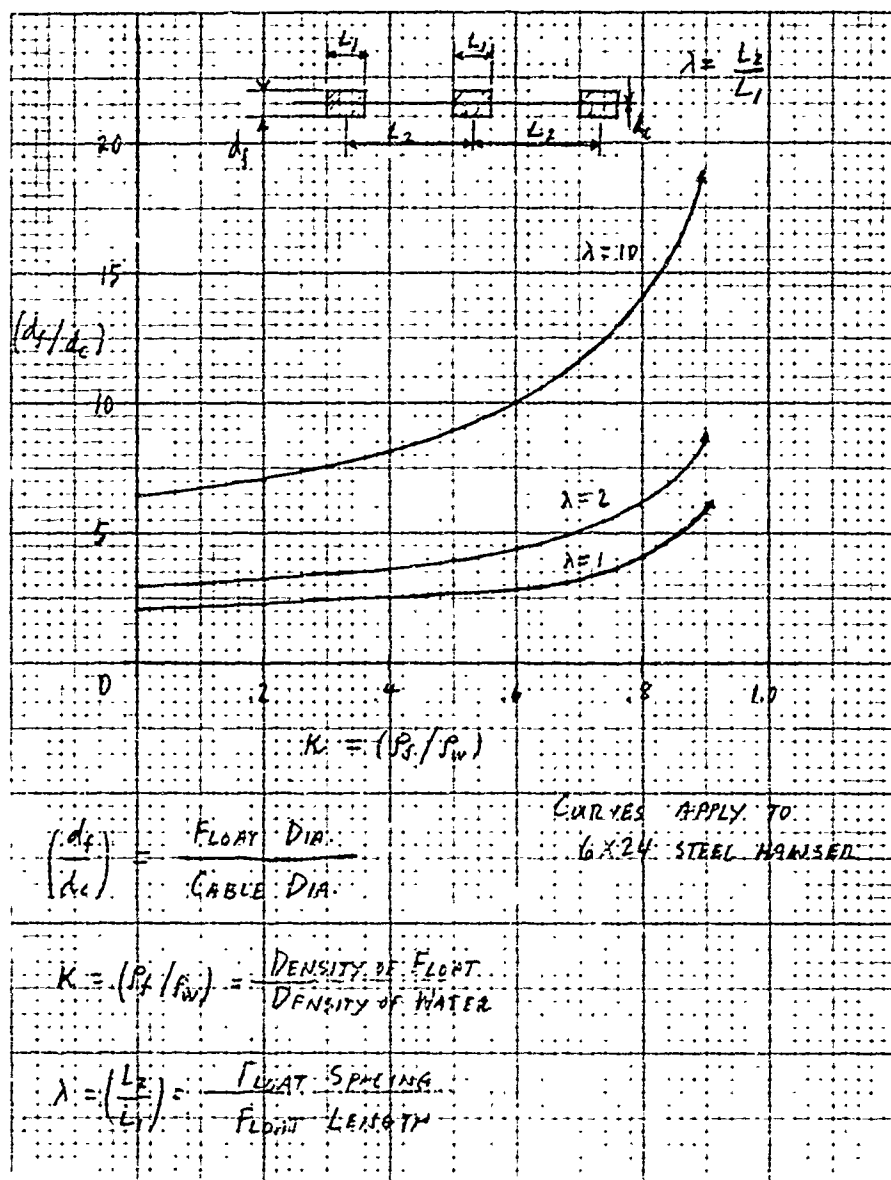
Figure 11. Float Size and Spacing

23

In the following section we examine the deflection response of a tripod to (1) changes in the cable and (2) loading parameters selected according to the material of the present section.

3. PARAMETRIC INVESTIGATION

In this section we examine the deflection response of a symmetrical tripod to changes in the cable and loading parameters. This deflection response is characterized by the horizontal and vertical deflections of the common cable joint. The cable movements may be calculated once this is known, but results relative to these movements are not presented.

Most of the results apply to a fixed tripod geometry 4000 feet high, and the order of magnitude of the deflections (1 to 20 feet) should be interpreted relative to this height. Our primary concern is the relative change in magnitude of these deflections with changes in the cable and loading parameters. Absolute magnitude of deflections should be interpreted carefully.

3.1 Current Velocity and Direction

For a fixed configuration (h = 4000 feet, d = 4000 feet, Lift = 100 kips) we have investigated the influence of current velocity and direction on the tripod deflections, while varying the buoy drag independently. These results are illustrated in Figure 12 where the horizontal deflection is plotted as a function of buoy drag for various values of current velocity and direction.

We observe two significant features:

1. The relative magnitudes of the deflections are not strongly dependent upon current velocity and direction

2. For small values of buoy drag there is a "sway-back" of this structure (i.e., the deflection is opposite to the current direction).

3.1.1 Remark 1. The "sway-back" phenomenon in a bipod may be illustrated by a very simple analogy. Consider the combined gravity and current loadings on the bipod cables in Figure 12b. The magnitude of the resultant loading on cable A is greater than that on cable B. An analogous situation is illustrated in Figure 12c where a weight (constant lift) is suspended by two light strings (A, B). If we push on string A and pull lightly on string B as shown, the common joint will move to the left; in effect, opposite to the current direction. As the buoy drag is increased, the joint moves in the stream direction.
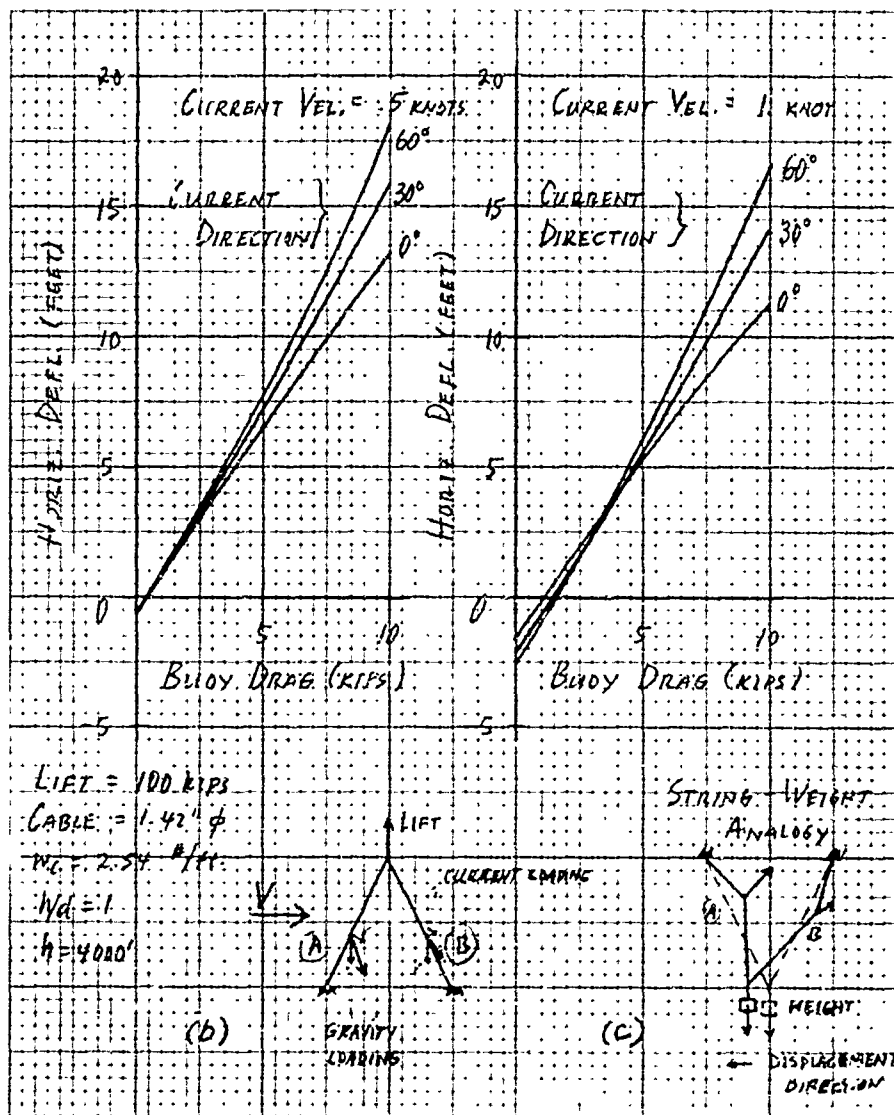
24

Figure 12. Influence of Current Velocity and Direction

3.2 Cable Parameters

In this subsection we examine the deflection dependence on the extensibility k_c and weight-in-water w_c of the cables. The most obvious result is the variation in vertical deflection under the lift force due to changes in k_c. This situation is illustrated in Figure 13a where $k_c = 0$ corresponds to inextensible cables and $k_c = 3.3 \times 10^{-5}$ is roughly the value for 1-7/16 inch ω steel hawsers. The most significant feature displayed in Figure 13a is not the absolute differences in values of the
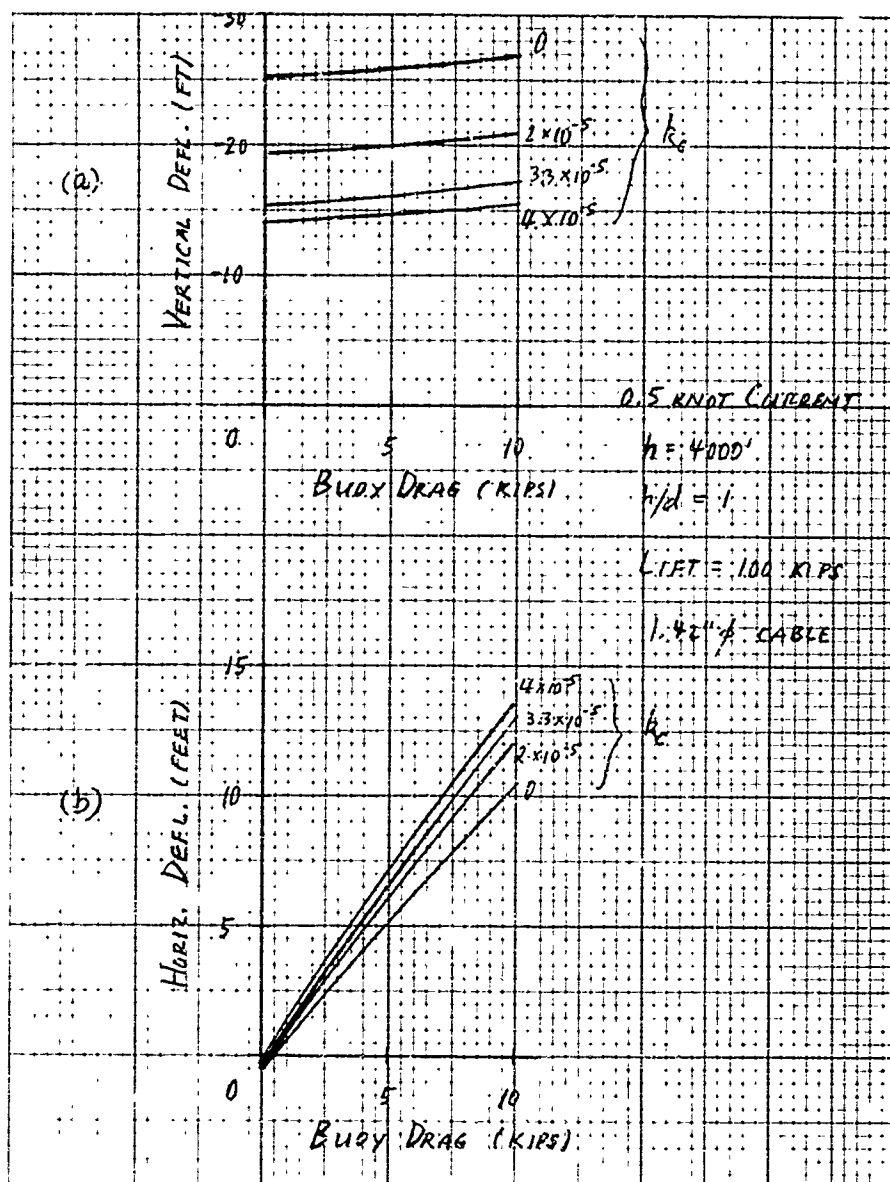
Figure 13. Influence of Cable Extensibility

vertical position but the dependence of the respective vertical deflections on the buoy drag. This variation is quite small when compared with the results for the horizontal deflection shown in Figure 13b.

Remark 2. We should remember that the nominal joint position is determined by the lift force and cable weight. Deflections from this position caused by additional loadings and environment induced changes are items of interest.

The effect of reducing the cable weight-in-water w_c has considerably more significant influence on the joint deflection than changes in k_c. These results are shown in Figure 14 where w_c was varied while holding the lift and buoy drag constant. The deflections corresponding to inextensible cables are given by the dashed lines, and those corresponding to $k_c = 3.3 \times 10^{-5}$ are given by the solid lines. We observe that for a buoy drag of 10 kips the effect of rendering the cable neutrally buoyant is a decrease in horizontal deflection of approximately 10 feet or 80 percent.
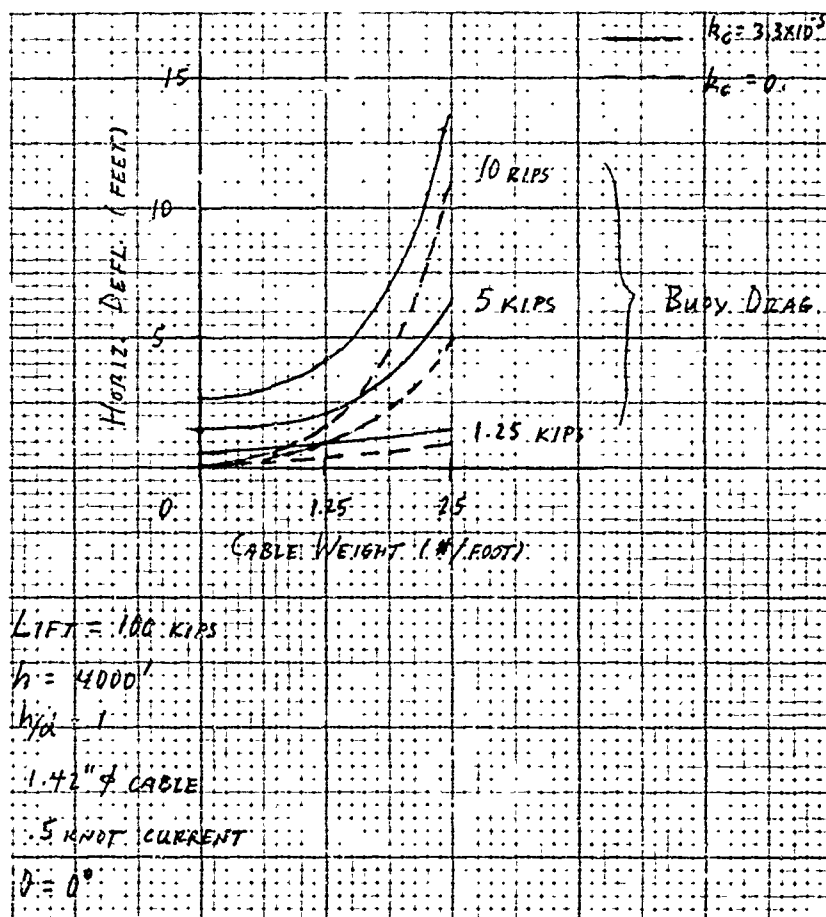
Figure 14. Influence of Cable Weight

Remark 3. The effect of cable weight on the horizontal deflections is the most significant result observed in the present numerical studies. It would seem that floated cables would be required in applications where very small deflection tolerances (~ few feet) are necessary and the buoy drag is appreciable (~ 5 kips).

27

3.3 Buoy and Lift Drag

In Figure 15 we show the effect of changes in lift force on the deflection response of the structure (for fixed buoy drag). The solid line refers to the situation where the normal design weight of the cables is included in the calculation and the dashed line assumes that neutrally buoyant cables are employed.
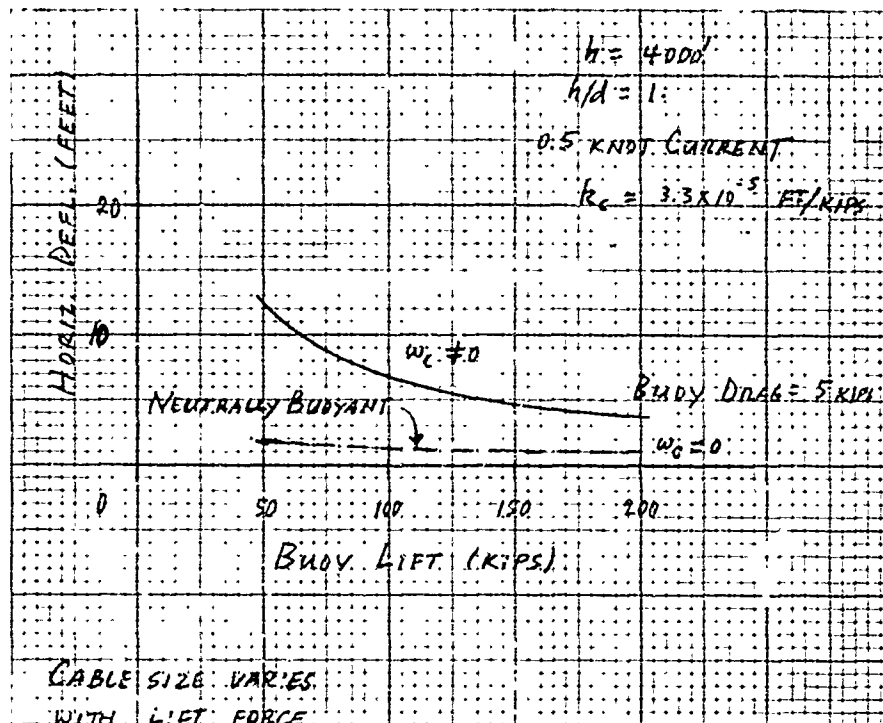

Figure 15. Influence of Buoy Lift

It is seen that in the neutrally buoyant case the horizontal deflection is only slightly dependent upon the lift force. Independent analytical and numerical checks also indicate that the deflection depends very little upon the current loading.

Remark 4. If buoy lifetime were a critical element in the system design, floated cables and multiple buoys (say, three buoys providing 50 kips lift each) would preserve the horizontal deflection response of the structure against buoy failure (see Figure 15).

28

3.4 Geometry

In the deflection-limited design of a buoy tripod system we can look for the minimum-deflection structure under specified loading conditions and fixed height. The present study has not been extensive enought to investigate this situation when cable weight-in-water is considered. However, for floated cable systems we can make some definitive statements.

An analytical investigation by the author for the tripod systems, ignoring distributed loadings, showed that the minimum-horizontal deflection structure has a ratio $h/d \approx 0.7$. This result is almost independent of the height h, lift force, and buoy drag.

We checked this result numerically for a tripod with fixed h, lift, and buoy drag, considering current loading on the cables. The results for various h/d are shown in Figure 16. We found that the minimum deflection did occur for $h/d \approx 0.7$ but that this was a very weak minimum.
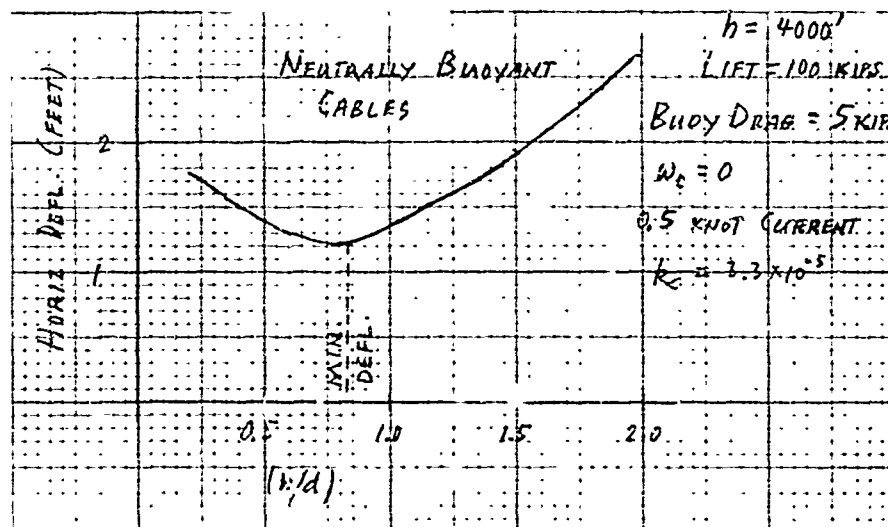
Figure 16. Influence of Geometry

4. SUMMARY AND RECOMMENDATIONS

In this report we have examined the deflection response of buoyed tripods to current loading, and identified the most significant factors that determine variations in this response. We are presently developing an analytical solution for the tripod, considering weight and current loadings. This will be available for more extensive

parametric studies and will allow a more complete investigation of the deflection response to cable weight.

It is recommended that the proposed applications of buoyed tripods be delineated more closely so that deflection-limiting criteria may be established. We also suggest that variations in placement conditions affecting the symmetry of the tripod be examined and that temporal variations in the loading conditions be considered.

Part III

DYNAMICS OF A MOORED RIGID BODY

Knowledge of the motions of a large, buoyant, rigid underwater structure is important for underwater sound applications. In this report we consider such a structure and its motions as determined by numerical quadrature of the linearized equations of motion.

The purpose of a study of the dynamic response of large moored under water structures is to determine approximately the following properties: (1) the "settling time" required for the structure to adjust to changes in ambient current; (2) the amplitude of attitude motions in response to initial conditions or disturbances from trawlers and ground motion; (3) the linearized static displacements of the structure when subjected to steady current loading.

To achieve these aims, we have neglected such factors as flexibility of the structure and current loading on the anchor cables. These assumptions should not alter the approximate response and are necessary for an efficient preliminary analysis. The validity of the linearized equations of motion was established by a posteriori checks.

1. ASSUMPTIONS

First, we set up a general dynamical description of an underwater, moored rigid body. Consider a body B_0 with a center of mass C_0 and a center of buoyancy C_B. Figure 17 shows the geometry of the body with the ith mooring cable K_i in place. An inertial reference frame R is established on the ocean bottom; the anchor point of K_i is denoted by P_{B_i}, a vector distance $\underline{b}^i$ from R. The length vector of K_i is $\underline{\ell}^i$ from P_{B_i} to P_{A_i}, the point of attachment of the cable and body B_0. The vector from C_0, the center of mass of B_0, to P_{A_i} is $\underline{\rho}^i$; the center of buoyancy C_B is a distance $\underline{\ell}^B$ from C_0. The buoyant force W_b, equal to the volume of B_0 times the density of water, is active at point C_B.

The angular velocity of B_0 expressed in a body-fixed reference frame is given as $\underline{\omega}$. The position $\underline{r}$ of C_0 relative to R is broken into $\underline{r}^\circ$ the static position and $\Delta\underline{r}$ the dynamic displacement from equilibrium.
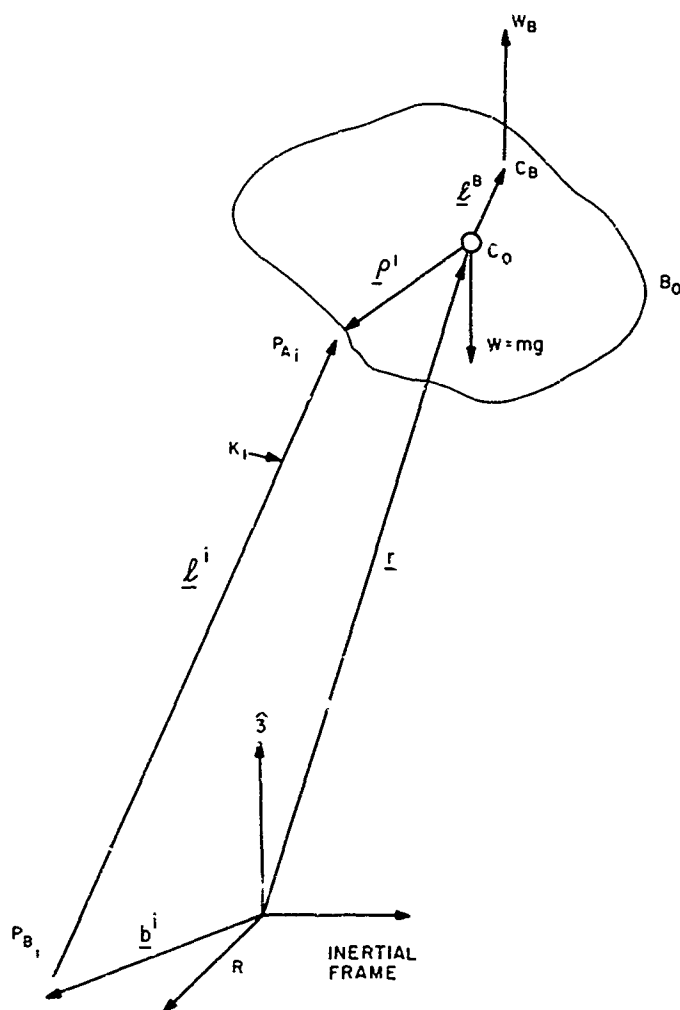
31

Figure 17. Geometry
of Mooring

2. EQUATIONS OF MOTION

The equations of motion of the system as defined are

$$
m\Delta\ddot{\underline{r}} = \underline{D} - \sum_{i=1}^{N_c} \underline{F}^i + \left(W_b - W\right)\hat{3} \tag{1}
$$

$$
\dot{\underline{H}} = \underline{L}^d - \sum_{i=1}^{N_c} \underline{\rho}^i \times \underline{F}^i + W_b \underline{\ell}^B \times \hat{3} \tag{2}
$$

where $\underline{H} = I \cdot \underline{\omega}$, I is the inertia dyadic. $\underline{D}, \underline{L}^d$ are the hydrodynamic drag force and moment, N_c is the number of cables, and $\hat{3}$ is along the earth's radius. The force $\underline{F}^i$ is the force acting on the cable K_i.

32

We must now compute $\underline{F}^i$, $\underline{D}$, $\underline{L}^d$ according to the laws of physics and certain assumptions. The geometry of the cable is given by $\underline{\ell}^i = \underline{r} + \underline{\rho}^i - \underline{b}^i$.

3. MOORING FORCE

For a close approximation we neglect the weight and current reaction on the cables. These effects are statically significant, but dynamically of secondary importance compared with the longitudinal elasticity effect.[*] We apply Hooke's law to the cable. The reaction force $\underline{F}^i$ on K_i is in the direction of the total length $\underline{\ell}^i + \Delta\underline{\ell}^i$, where now we use quantities at equilibrium plus their dynamic displacements; e.g., $\underline{r}^\circ + \Delta\underline{r}$ is written $\underline{r} + \Delta\underline{r}$. Figure 18 shows the simple geometry. The cable tension-per-foot-deflection based on an unstressed length ℓ^{si} is given as N_i. The "stressed cable" reaction force is

$$\underline{F}^i + \Delta\underline{F}^i = N\left(|\underline{\ell}^i + \Delta\underline{\ell}^i| - \ell^{si}\right)\frac{\Delta\underline{\ell}^i + \underline{\ell}^i}{|\Delta\underline{\ell}^i + \underline{\ell}^i|} .$$

The static force is

$$\underline{F}^i = N\left(|\underline{\ell}^i| - \ell^{si}\right)\left(\frac{\underline{\ell}^i}{|\underline{\ell}^i|}\right) .$$

Linearity and the notation

$$T_o = N\left(|\underline{\ell}^i| - \ell^{si}\right)$$

gives

$$\Delta\underline{F}^i = \frac{N\left(\underline{\ell}^i \cdot \Delta\underline{\ell}^i\right)\underline{\ell}^i}{|\underline{\ell}^i|^2} + T_o\left(\frac{\Delta\underline{\ell}^i}{|\underline{\ell}^i|} - \frac{\Delta\underline{\ell}^i \cdot \underline{\ell}^i}{|\underline{\ell}^i|^3}\underline{\ell}^i\right) \tag{3}$$

up to order $|\Delta\ell^i|^2$. The last term is small compared with the first.

4. HYDRODYNAMIC DRAG

The drag on an arbitrarily oriented cylinder is calculated. The cylinders are then used to construct a large tetrahedron structure by joining four cylindrical

---

[*]In this report we are attempting to study dynamic reactions of a structure to current loading. Clearly the effects of current on the rigid body are largely due to loading on the body itself; this is because of the relatively large area of the body.
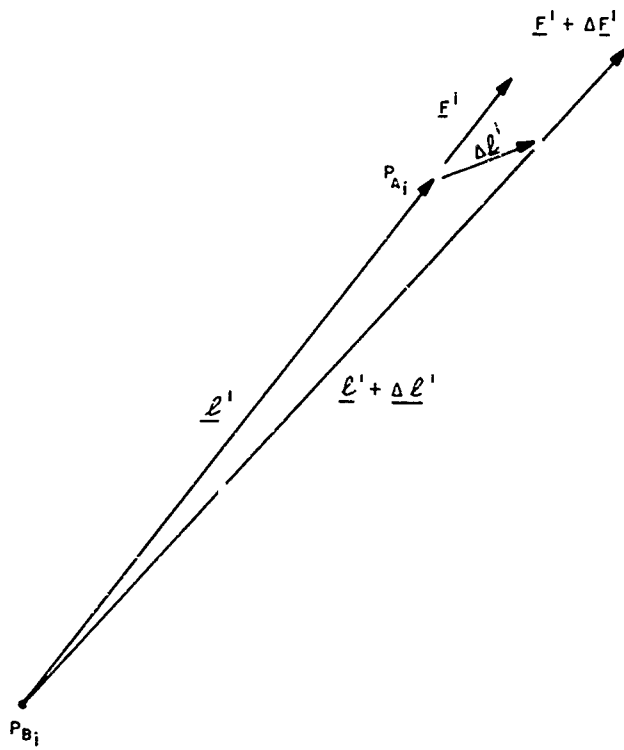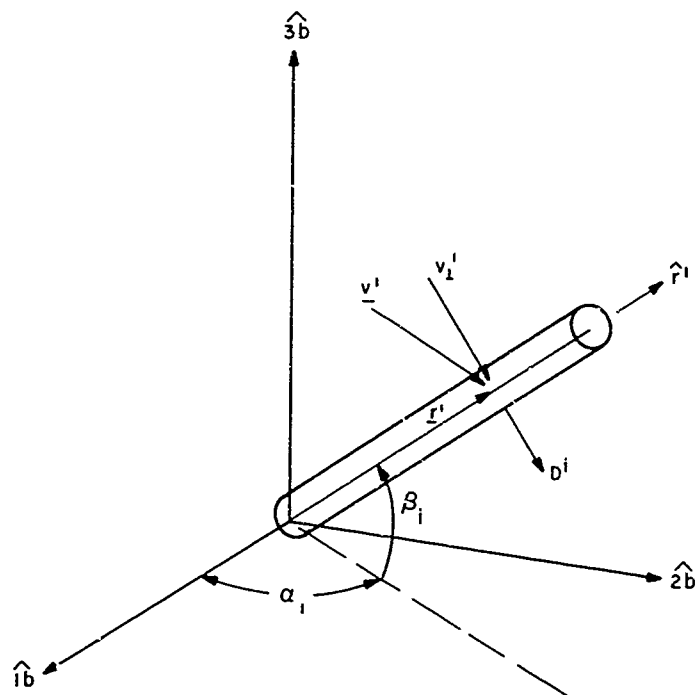
Figure 18. Mooring Cable Geometry

Figure 19. Drag Geometry

34

members at the origin (see Figure 19) by their ends and using tension members (cables) to complete the structure.

The axis of the cylinder is given by a vector $\underline{r}^i = r^i \hat{r}^i$ for the ith cylinder, where r^i is the distance from one end of the cylinder and $\hat{r}^i$ a unit vector. The prevailing current is given by the scalar v in a direction $\hat{u}$ (the carat denotes a unit vector). Consulting Figure 19 we assume the current velocity $\underline{v}^i$ composed of two parts: $\underline{v}^i_\perp$ perpendicular to $\hat{r}^i$ and $\underline{v}^i_{\parallel}$ along $\hat{r}^i$. Thus

$$v^i_\perp = P^i \cdot \underline{v}^i$$

where $P^i = (\hat{\hat{1}} - \hat{r}^i \hat{r}^i)$ is a dyadic and $\hat{\hat{1}}$ is the unit dyadic.*

The drag force $\underline{D}^i$ is an integration of the form

$$\underline{D}^i = \frac{\rho_w C_d d}{2} \int_0^{a_i} dr^i \left| \underline{v}^i_\perp \right| \underline{v}^i_\perp \ ,$$

where $v^i_\perp = P^i \cdot \underline{v}^i$ and $\underline{v}^i$ is a summation of current and motion effects:

$$\underline{v}^i = \left[v\hat{u} - \left(\Delta \dot{\underline{r}} + \underline{\omega} \times \underline{r}^i \right) \right] .$$

The torque about the origin on the ith cylinder is

$$\underline{L}^{di} = \frac{\rho_w C_d d}{2} \int_0^{a_i} dr^i \, r^i \left(\hat{r}^i \times \underline{v}^i_\perp \right) \left| \underline{v}^i_\perp \right| .$$

The length of the cylinder is given by a_i, the density of water by ρ_w, the drag coefficient by C_d, the cylinder diameter by d.

We then linearize $\underline{D}^i$ and $\underline{L}^{di}$ by assuming $v \gg |\Delta \dot{r}|$, $|\underline{\omega} \times \underline{r}^i|$.

5. SIMULATION: TETRAHEDRON ARRAY

Consider a rigid tetrahedron composed of cylinders as shown in Figure 20. The rigidity of the structure derives from cables in tension against large cylindrical members. Cable mass and drag effects are ignored for the moment but can be added

---

*A "dyadic" is a pair of vectors (say $\underline{u}$ and $\underline{v}$) placed side by side. It has meaning when another vector is dot or cross multiplied by the dyad to form a vector or another dyad, e.g., $(\underline{uv}) \cdot P$, or $(\underline{uv}) \times P$.
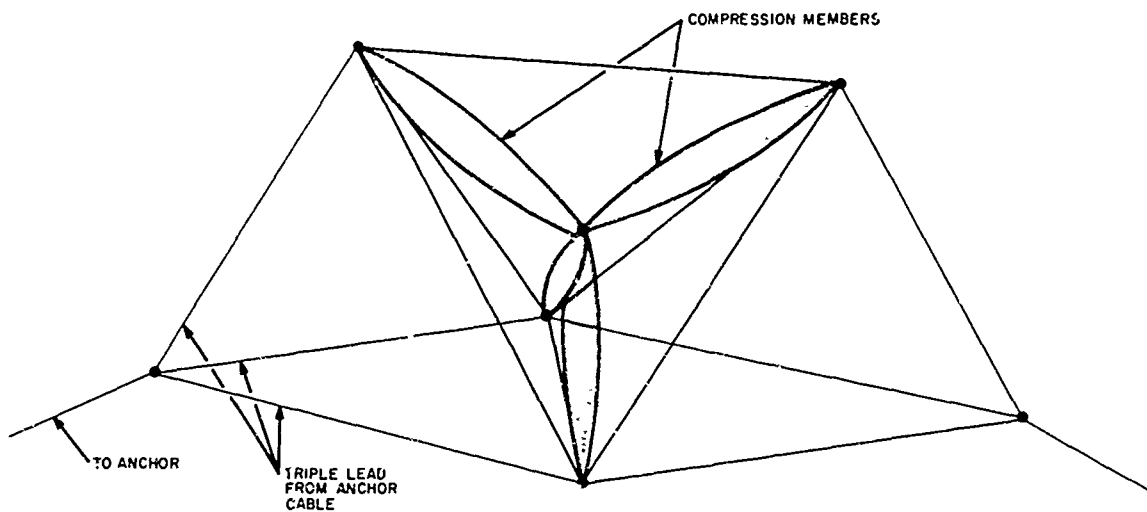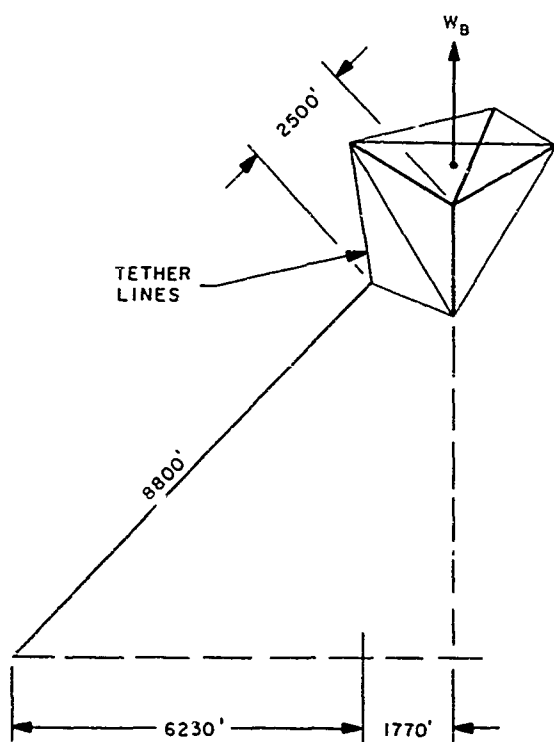
Figure 20. The Inverted Tetrahedron Concept

ℓ^B = DISTANCE FROM CENTER OF MASS TO CENTER OF BUOYANCY- 140 FT

W_B = BUOYANT FORCE 46,650,000 LB

W = WEIGHT IN AIR 150 000 LB

I_1 = 0.800 X 10^{12} SLUG FT^2

I_2 = 0 833 X 10^{12} SLUG FT^2

I_3 = 0 343 X 10^{12} SLUG FT^2
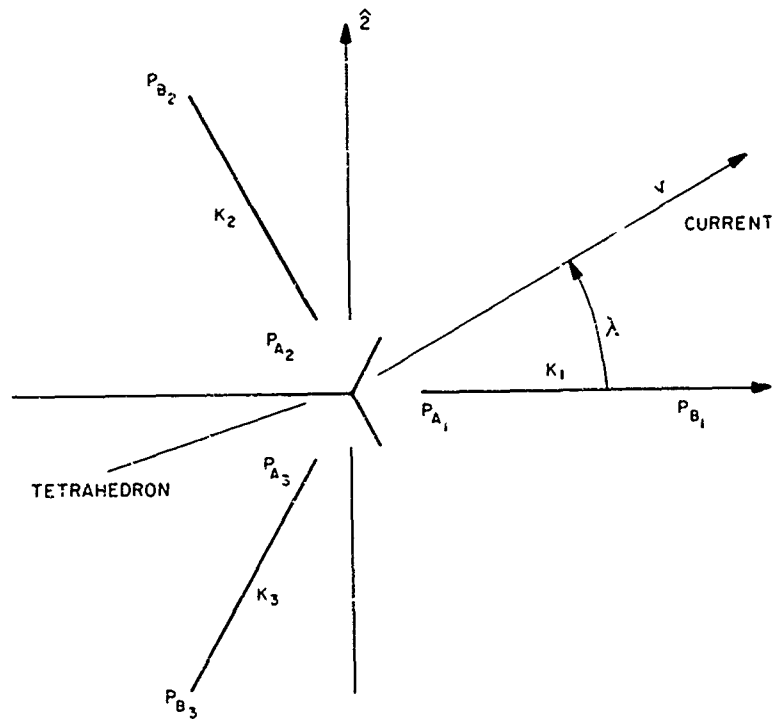
I_i = MOMENTS OF INERTIA

Figure 21. The Tetrahedron

36

Figure 22. Top View of Tetrahedron

to this rigid body analysis as changes in m, I, and the drag and drag moment equations, once a layout for guy wires and hydrophone suspensions has been specified.

We define a body coordinate frame with unit vectors $\hat{1b}$, $\hat{2b}$, $\hat{3b}$ describing the axes. This system is oriented by angles along the $\hat{1}$, $\hat{2}$, $\hat{3}$ system (inertial frame) for static equilibrium. The transformation matrix between a vector in $\hat{1}$, $\hat{2}$, $\hat{3}$ and one in $\hat{1b}$, $\hat{2b}$, $\hat{3b}$ is $\underline{V}_i = C \cdot \underline{V}_b$, where $\underline{V}_i$ and $\underline{V}_b$ denote representations of the same vector in the $\hat{1}$, $\hat{2}$, $\hat{3}$ and $\hat{1b}$, $\hat{2b}$, $\hat{3b}$ systems, respectively. The equation of motion (1) is expressed in the inertial frame and the equation (2) in the body frame.

The numerical integration of (1) and (2) was performed on the GE635 computer for a specific tetrahedron structure, using the DEPAK integration package. The vector operations were carried out automatically on the computer. Figure 21 shows the dimensions of the system studied. Figure 22 shows the top view of cable geometry and the current direction.

Figures 23 through 32 show a series of computer-plotted response curves. The odd-numbered figures are plots of the deflections Δx, Δy, Δz versus time (in seconds) and the even-numbered figures are of the angles γ_1, γ_2, γ_3 of rotations about $\hat{1b}$, $\hat{2b}$, $\hat{3b}$ plotted versus time. The initial conditions: a one-knot current

and no initial angles, deflections, or time derivatives of these. The variables Δx, Δy, Δz go to an equilibrium configuration to accommodate various values of current angle of attack λ. The transients in attitude are in every case less than 1 degree.

There is a simple empirical law of deflection for the structure as shown in Figure 33. The total deflection, $\sqrt{(\Delta x)^2 + (\Delta y)^2}$, is approximately constant at 17.5 feet for a one-knot current. The direction of this displacement is, to within a few degrees, equal to λ. For every 60 degree interval in λ the pattern repeats itself because of structural symmetry.

Figures 34 through 39 show plots of dynamic response with a one-knot current and initial conditions on the angles* $\gamma_1 = 0.01$ (Figures 34 and 35), $\gamma_2 = 0.01$ (Figures 36 and 37) and $\gamma_3 = 0.01$ (Figures 38 and 39). The initial conditions are imposed one at a time as can be seen from the rather marked attitude response due to the initialized angle. This attitude response shows noticeable damping in all cases and the translatory deflection approaches 17 feet as before (here $\lambda = 0^\circ$).

6. CONCLUSIONS FOR THE TETRAHEDRAL STRUCTURE

The response curves are nearly self-explanatory. The deflections do not seem particularly large and the angular response, while not too well damped in γ_1 and γ_2, seems to disappear in about 200 seconds. The angles excited by current alone are remarkably small, indicating the possibility of using such a structure as the support for a set of array hydrophones.

7. SIMULATION OF THE MOTIONS OF A SPHERICAL STRUCTURE

The system to be discussed here is similar in many respects to the previous moored, rigid tetrahedron.

The drag force (using the notation of Figure 17) is independent of attitude angles. It is given by

$$\underline{D} = \frac{\zeta_W C_D \pi R^2}{2} \left(|\underline{U} - \Delta \underline{\dot{r}}| \right) \left(U - \Delta \underline{\dot{r}} \right)$$

where R is the radius of the sphere, $\underline{U}$ is the current vector, and $\Delta \underline{\dot{r}}$ is the sphere velocity relative to the earth. The drag provides a constant force plus a damping force. C_D for the sphere was set equal to one.

---

*The angles γ_1, γ_2, γ_3 represent infinitesimal rotations about $\hat{1b}$, $\hat{2b}$, $\hat{3b}$, respectively.
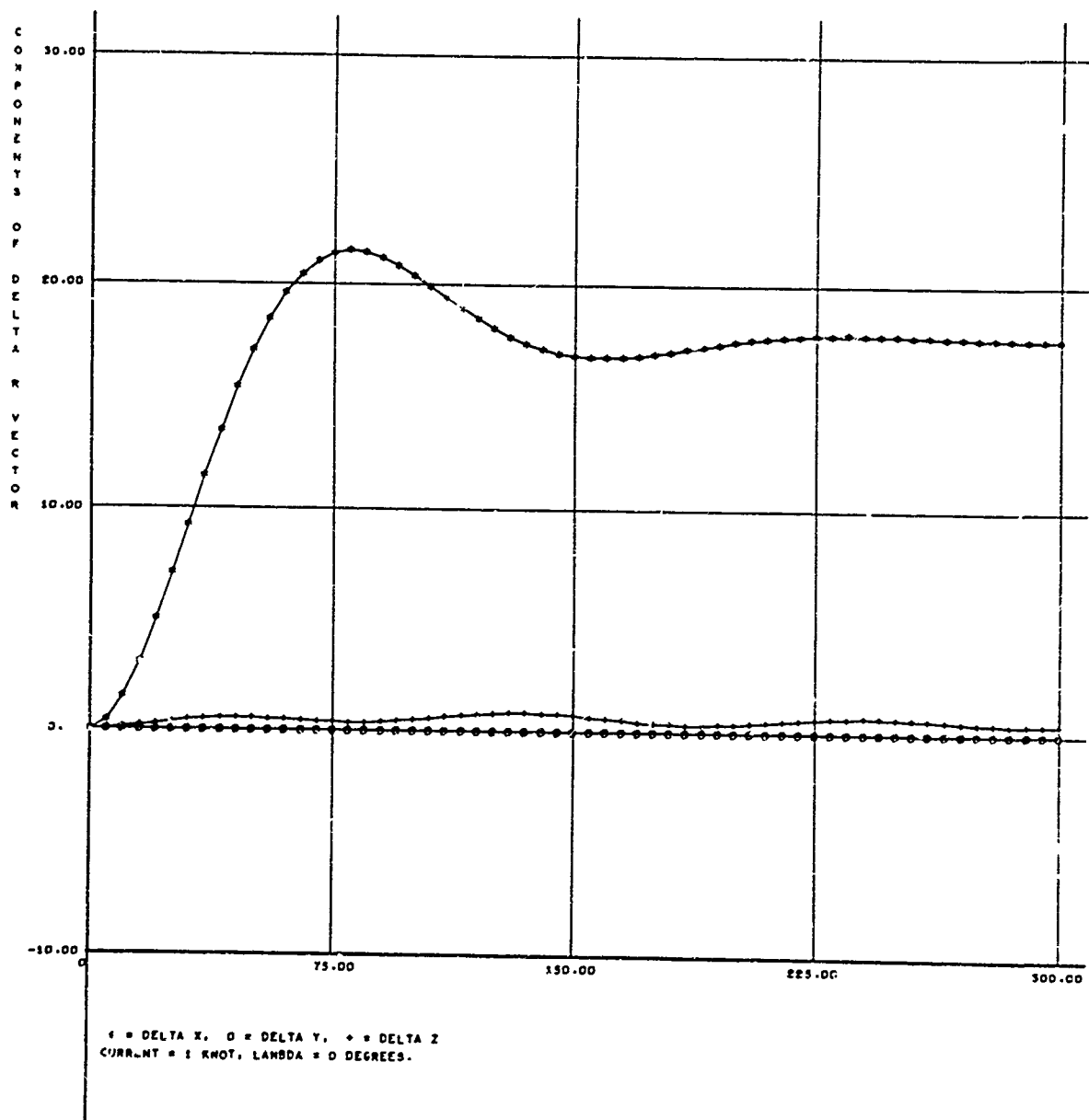
Figure 23. Plots of Delta X, Delta Y, and Delta Z Against Time
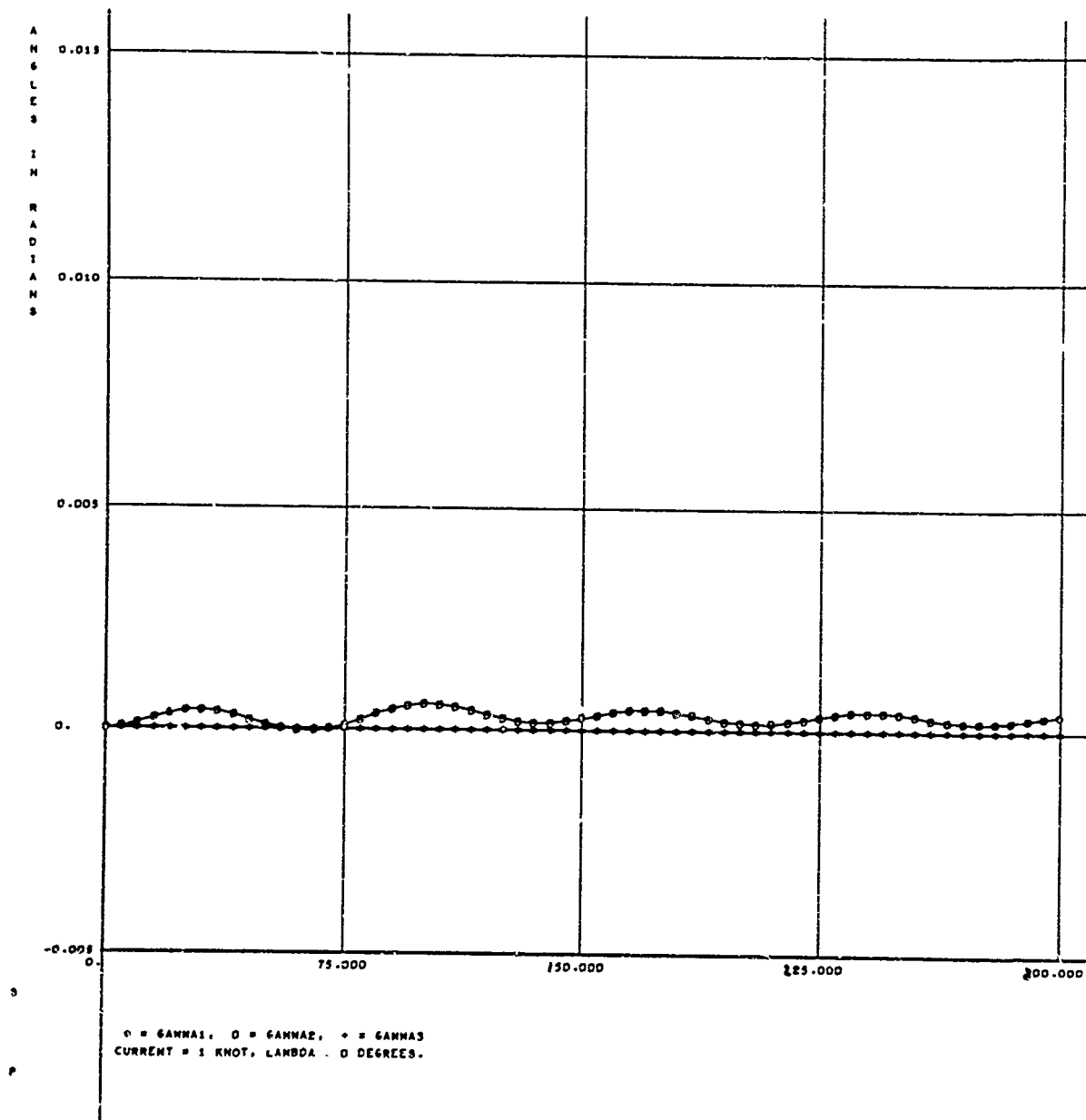
Figure 24. Plots of Gamma 1, Gamma 2, and Gamma 3 Against Time
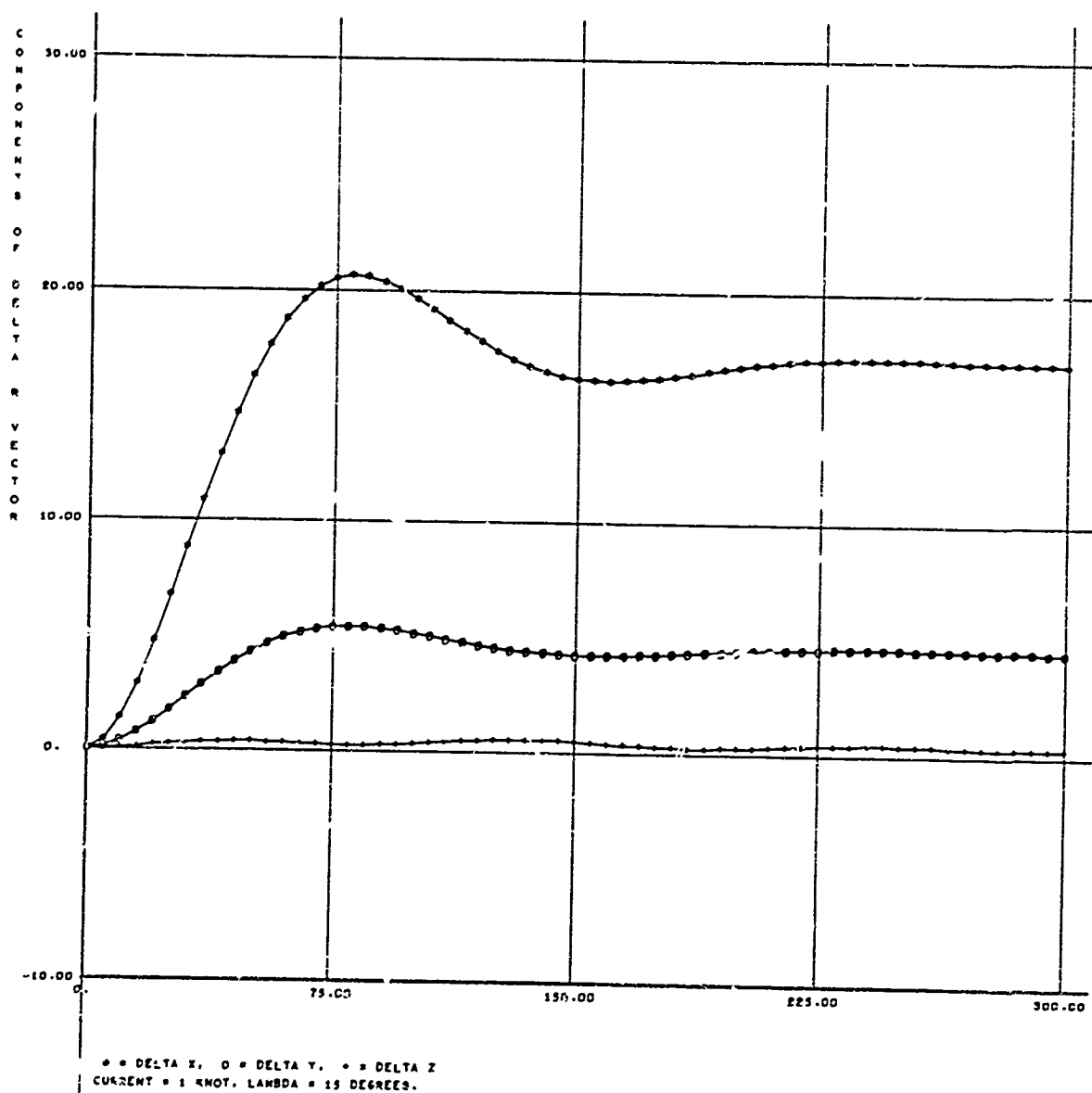
40

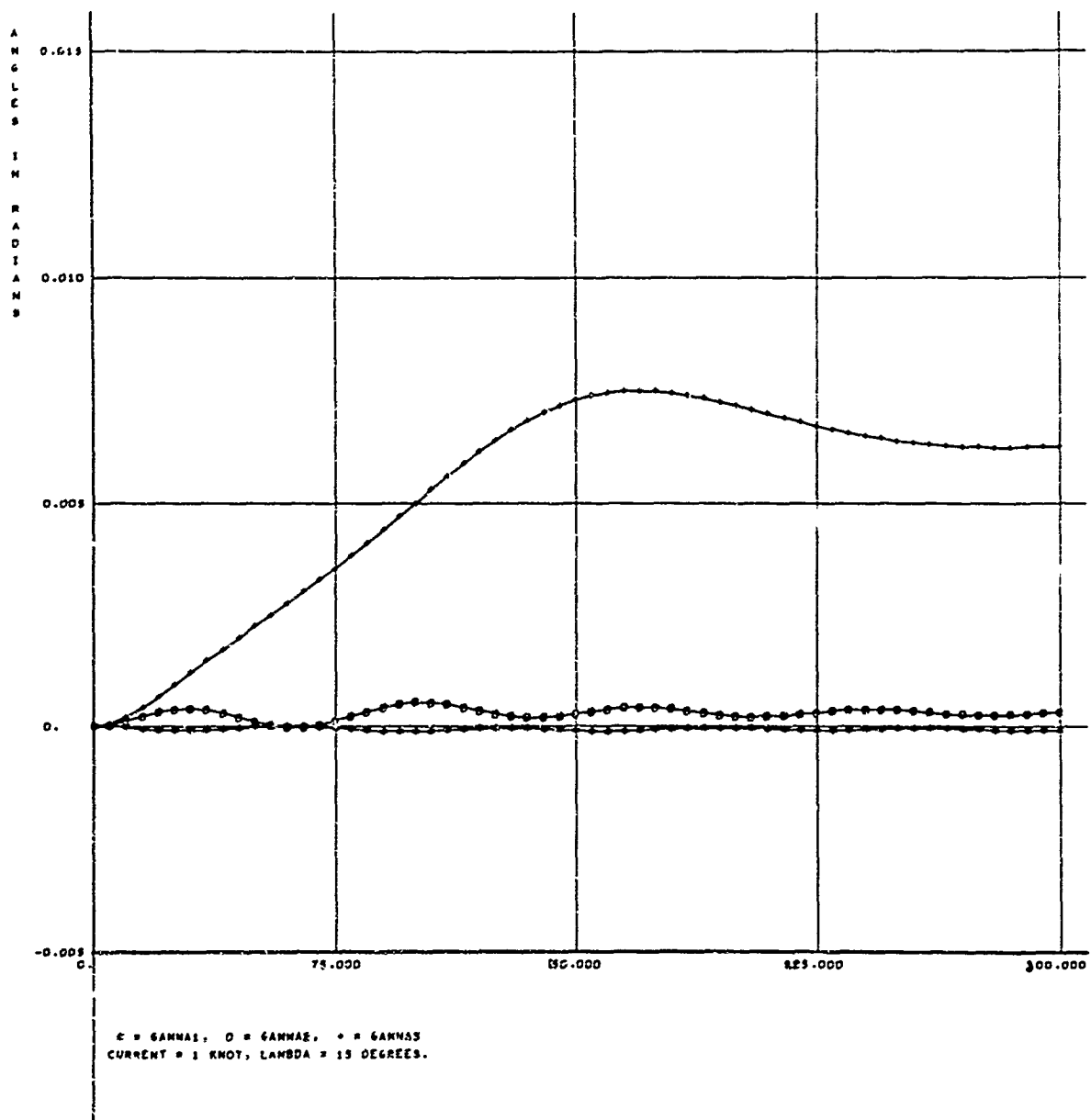Figure 25. Plots of Delta X, Delta Y, and Delta Z Against Time

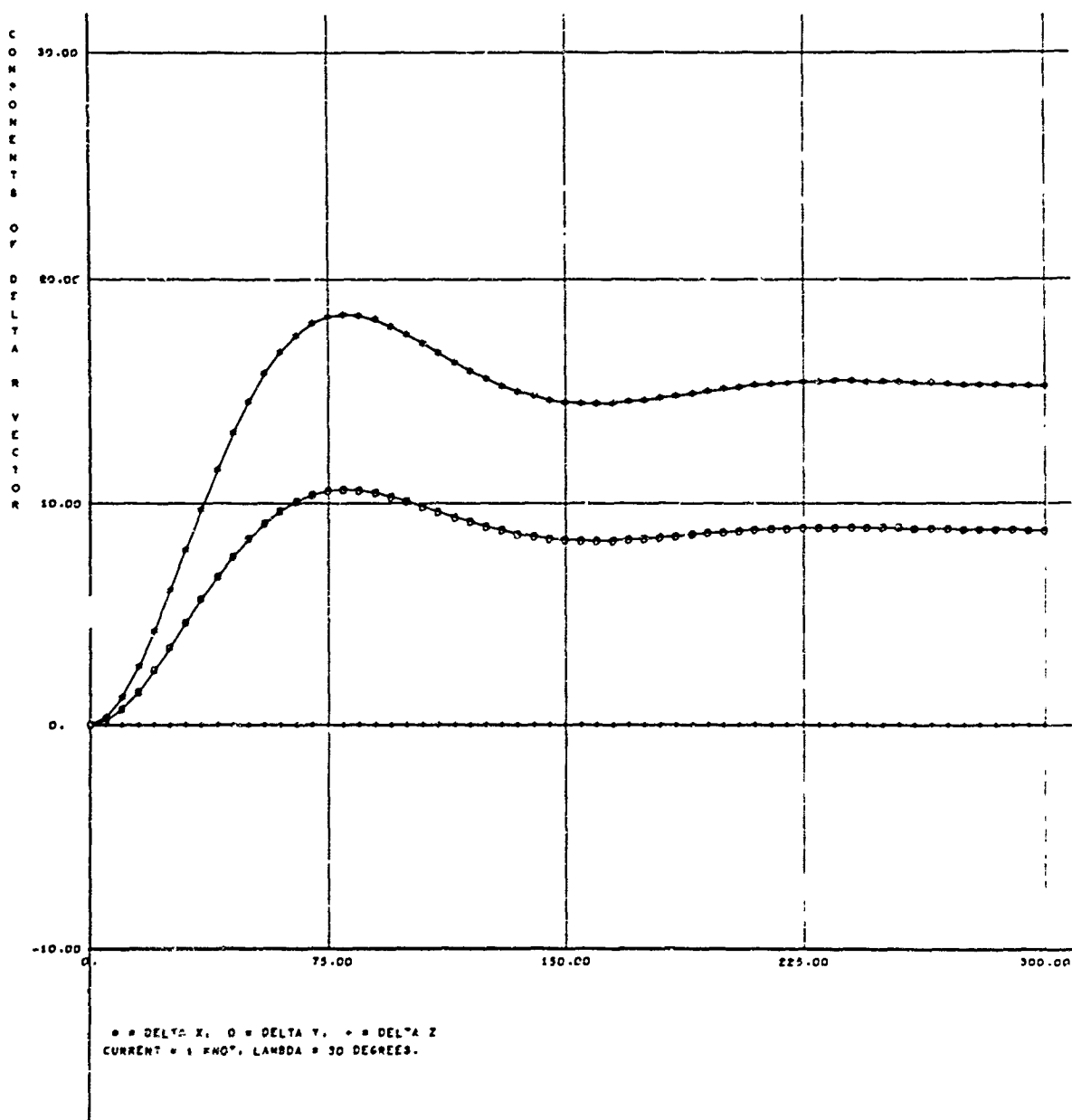Figure 26. Plots of Gamma 1, Gamma 2, and Gamma 3 Against Time

42

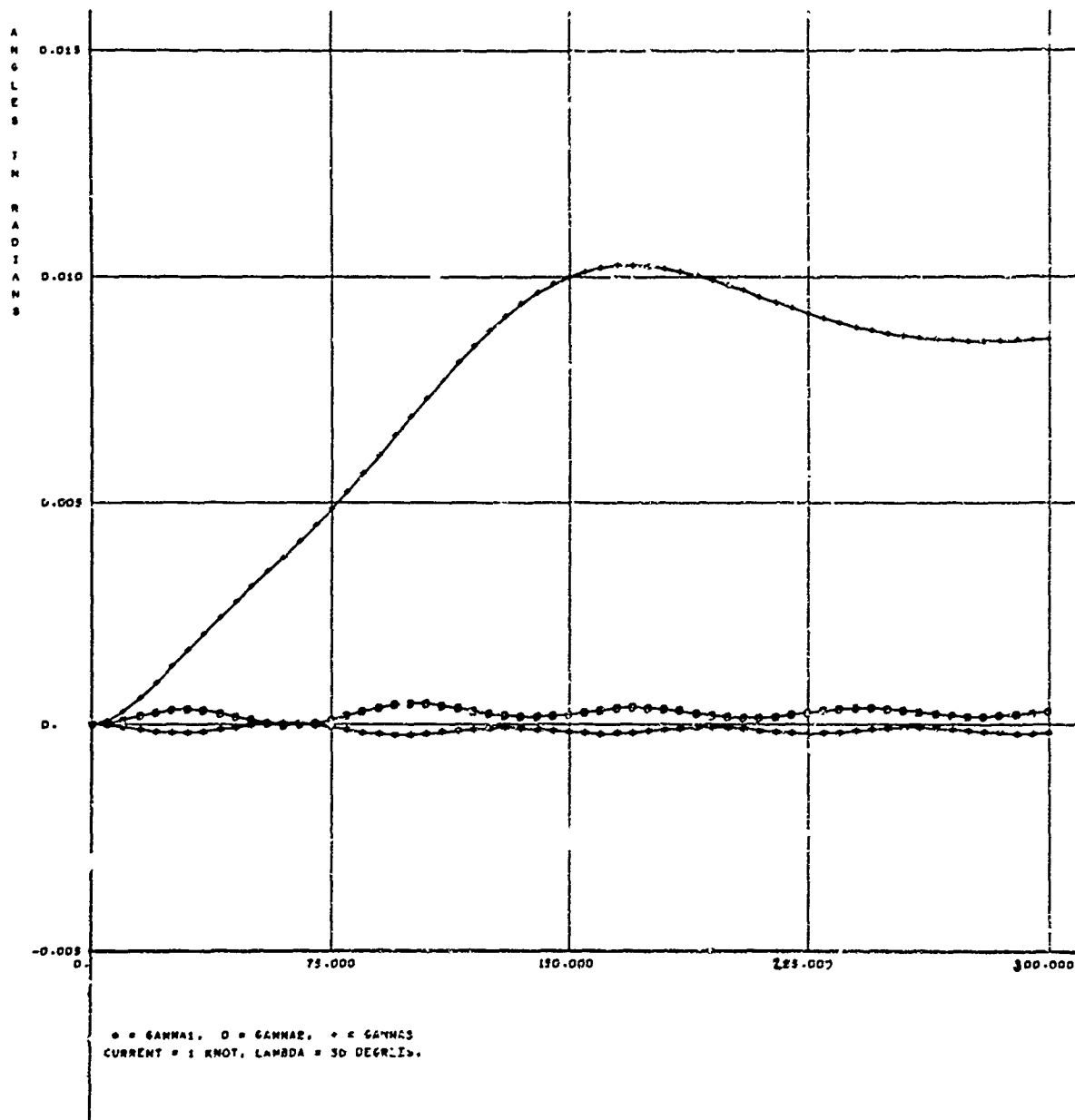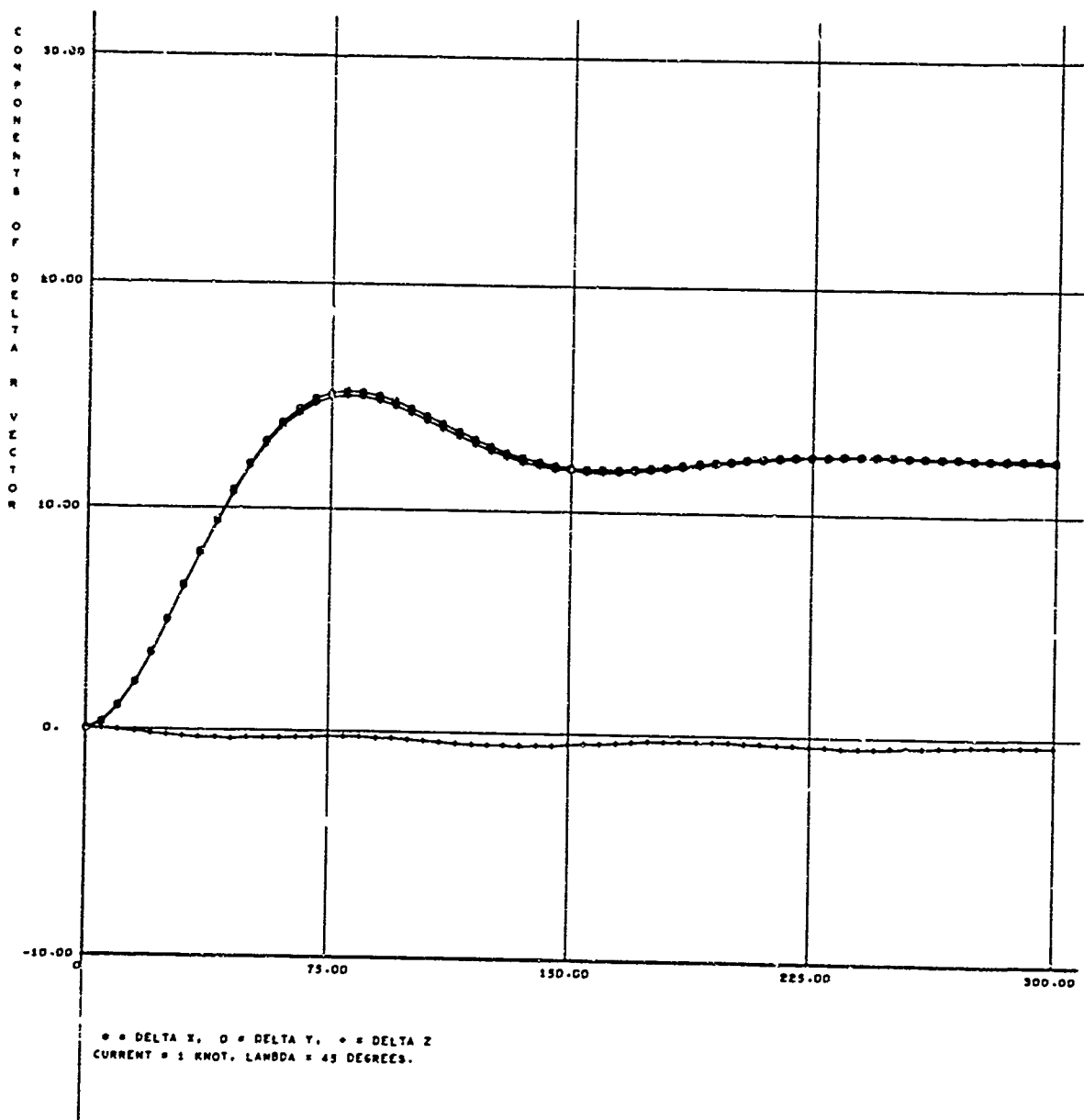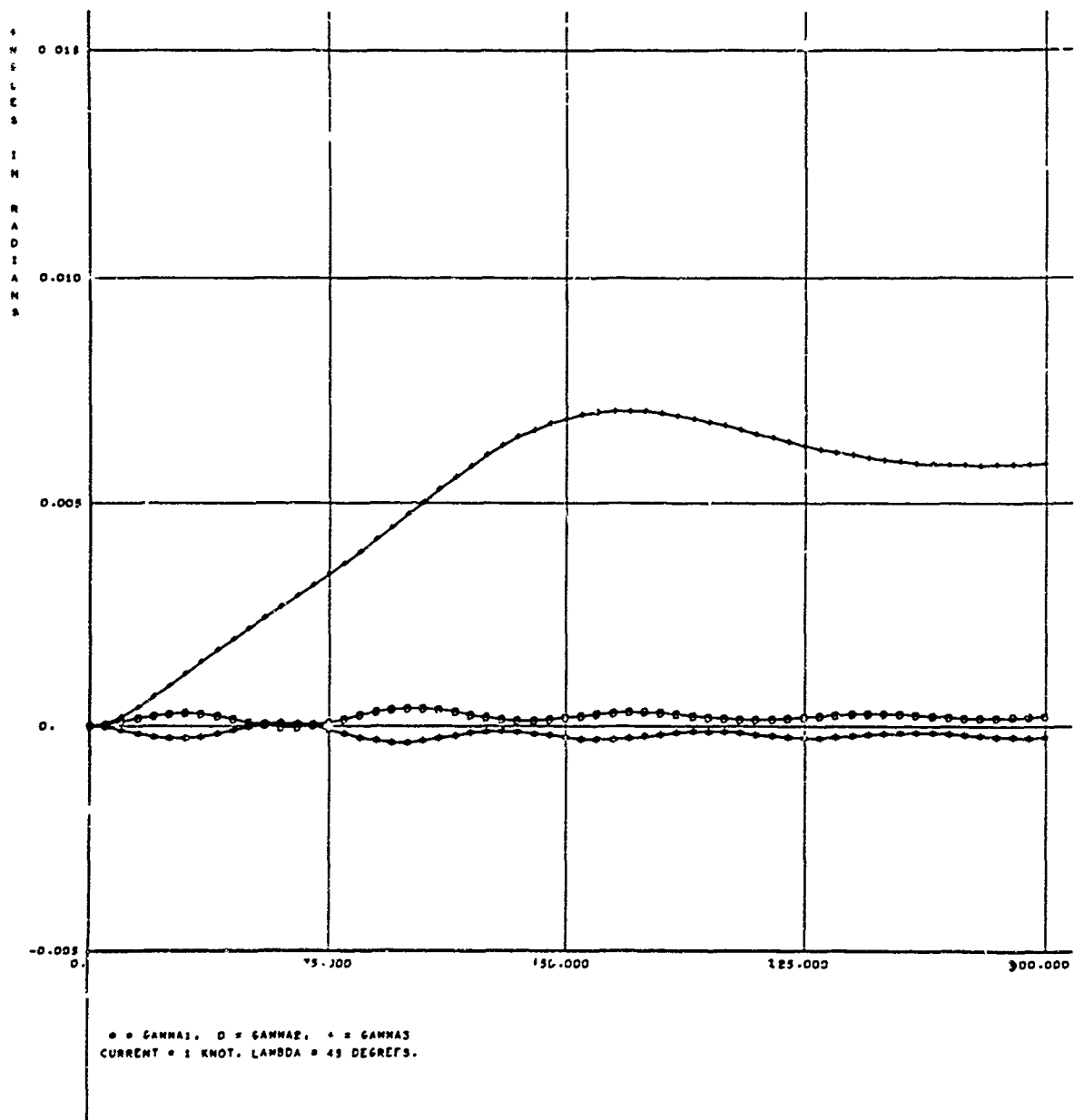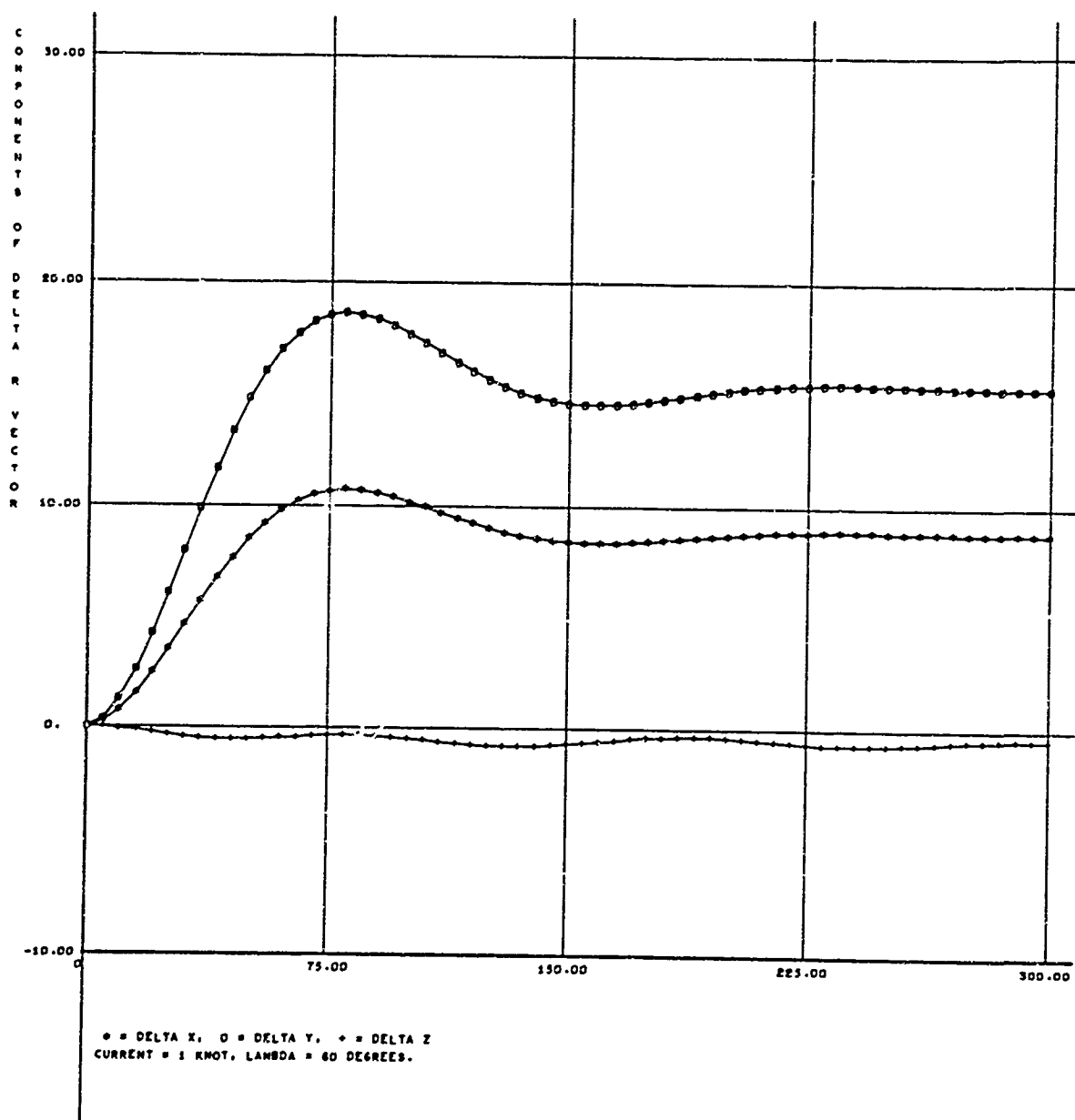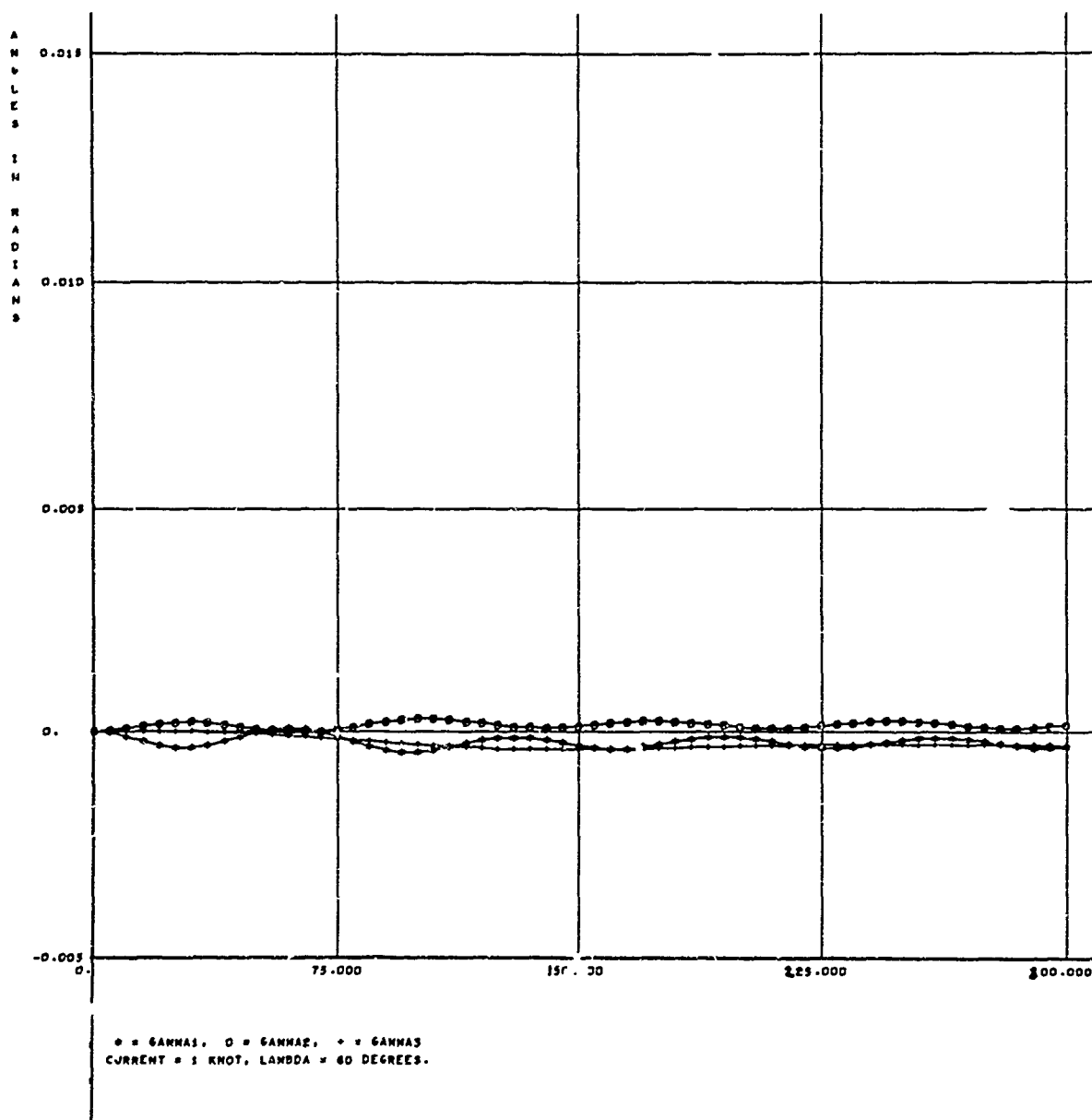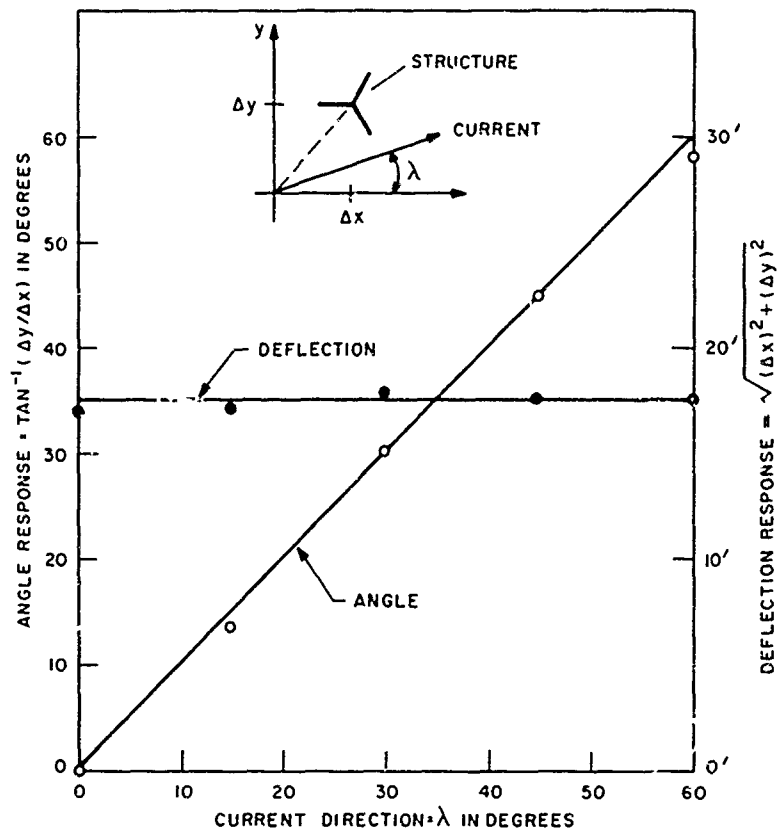Figure 27. Plots of Delta X, Delta Y, and Delta Z Against Time

43

Figure 28. Plots of Gamma 1, Gamma 2, and Gamma 3 Against Time

44

Figure 29. Plots of Delta X, Delta Y, and Delta Z Against Time

45

Figure 30. Plots of Gamma 1, Gamma 2, and Gamma 3 Against Time

46

Figure 31. Plots of Delta X, Delta Y, and Delta Z Against Time

47

Figure 32. Plots of Gamma 1, Gamma 2, and Gamma 3 Against Time

Figure 33. Response of Structure to a One-Knot Current

The mooring forces are provided by ten symmetrically spaced cables. These cables have the identical size and spring constant as those used previously for the tetrahedron and are fastened at the ocean bottom. About 800 feet from the top, each cable is joined to another cable of identical properties (see Figure 22). The main line is attached to the sphere at an elevation angle of 20 degrees above the sphere's equator, while the lower branch of each anchor line is tied to the lower pole of the sphere, providing stability.

For the system simulated, the buoyant force was to be $W_B = 2 \times 10^5$ pounds and the center of buoyancy was located 250 feet above the geometric center of a 500 foot radius sphere. The mass of the sphere was taken equal to the mass of the enclosed volume of water, i.e., $m = 0.8126 \times 10^{10}$ slugs. The moments of inertia of a typical spherical envelope were calculated to be 0.196×10^{10} slug-feet squared. Attitude damping equivalent to 10 percent was assumed to derive from internal parts of the sphere moving through water, and perhaps some artificial dampers (e.g., fins).
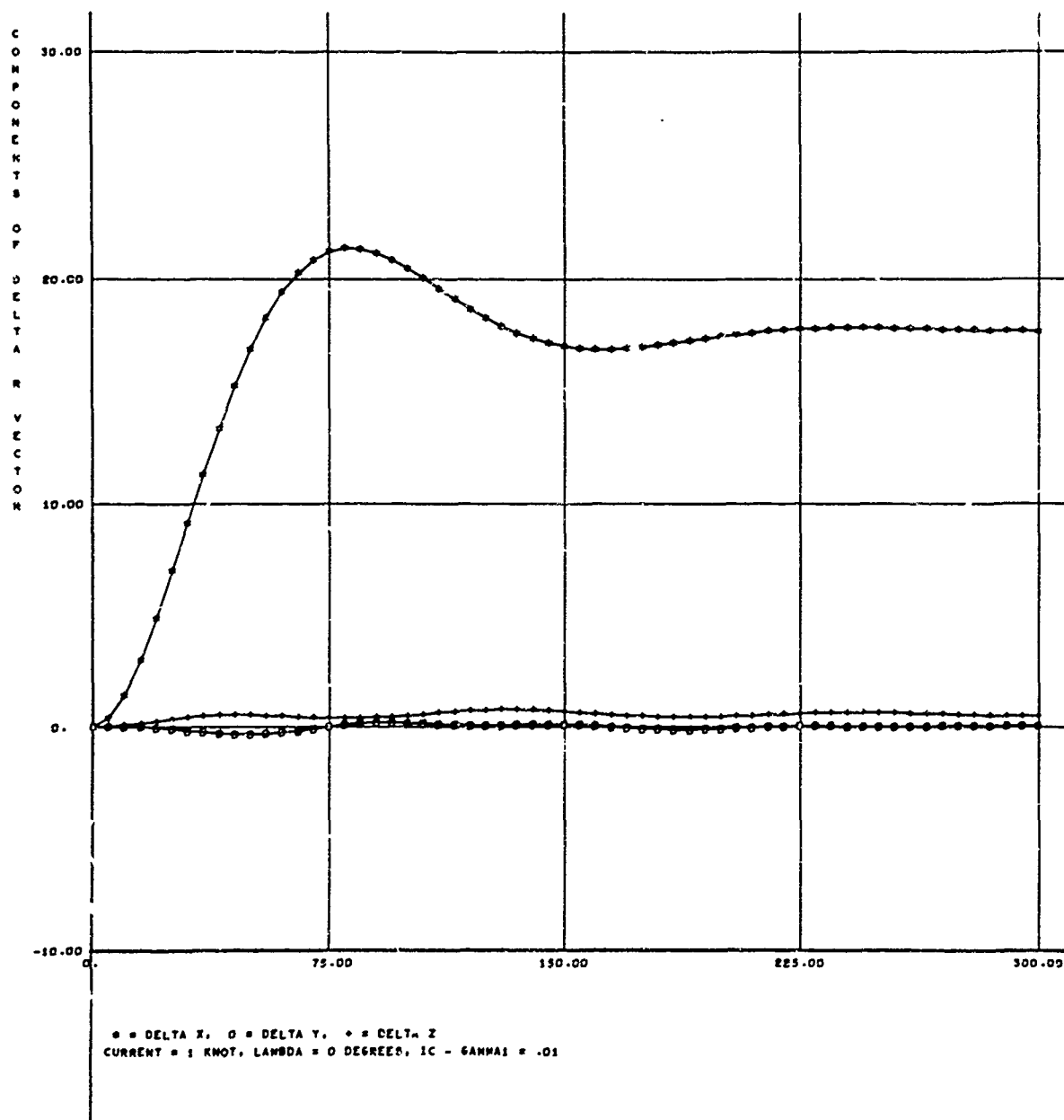
49

Figure 34. Plots of Delta X, Delta Y, and Delta Z Against Time
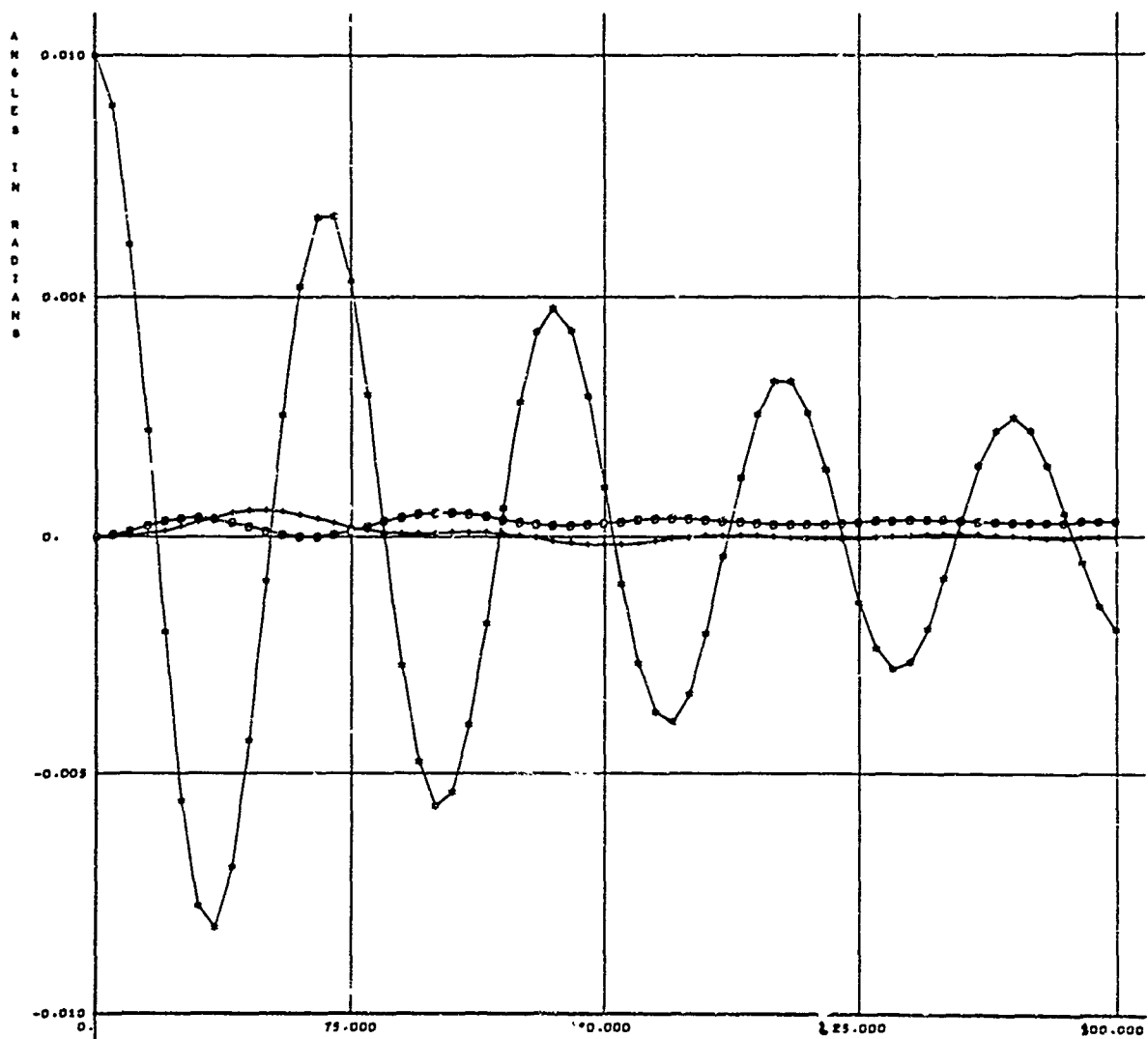
50

Figure 35. Plots of Gamma 1, Gamma 2, and Gamma 3 Against Time

● = GAMMA1, □ = GAMMA2, + = GAMMA3
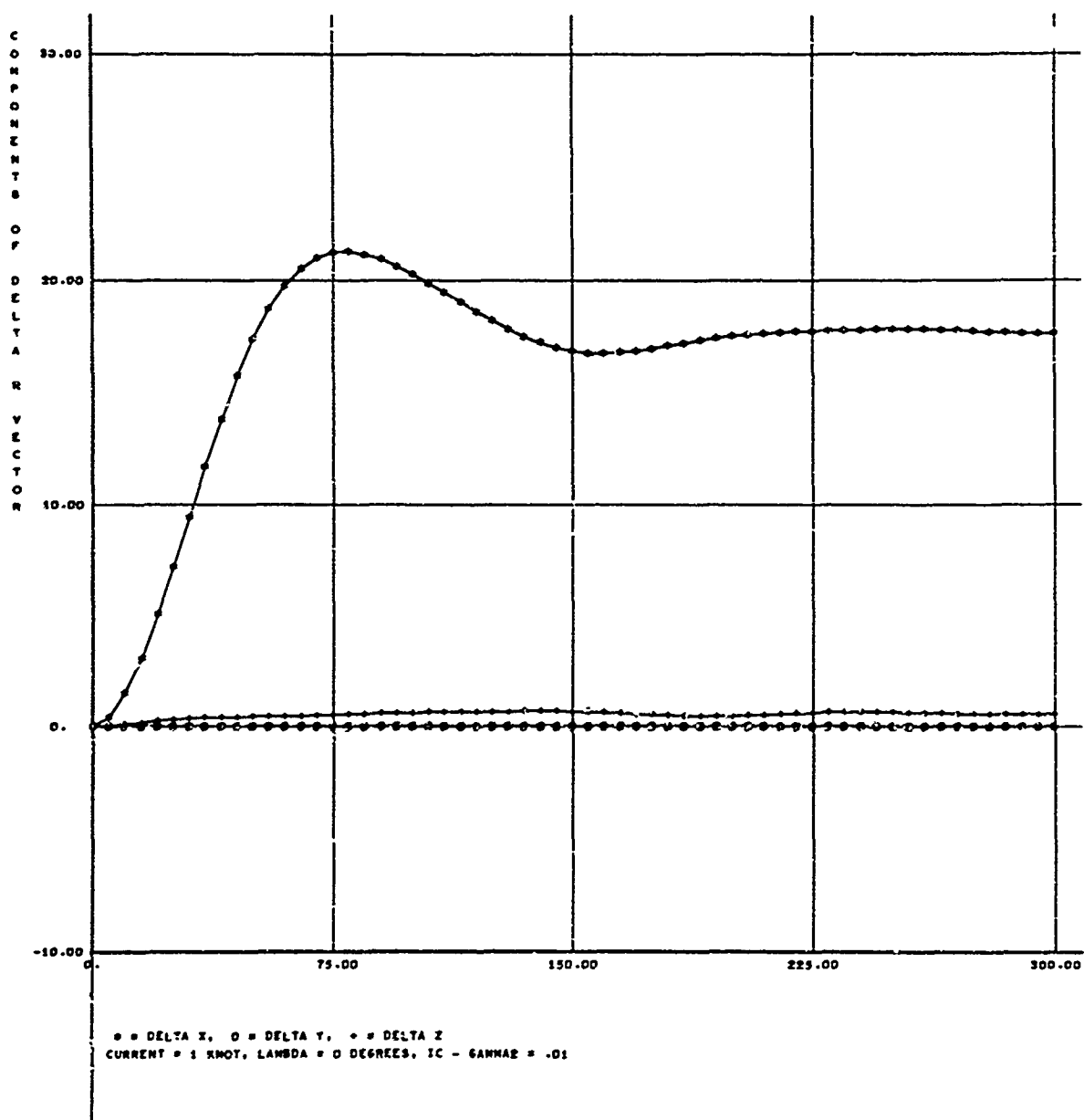CURRENT = 1 KNOT, LAMBDA = 0 DEGREES, IC - GAMMA1 = .01

51

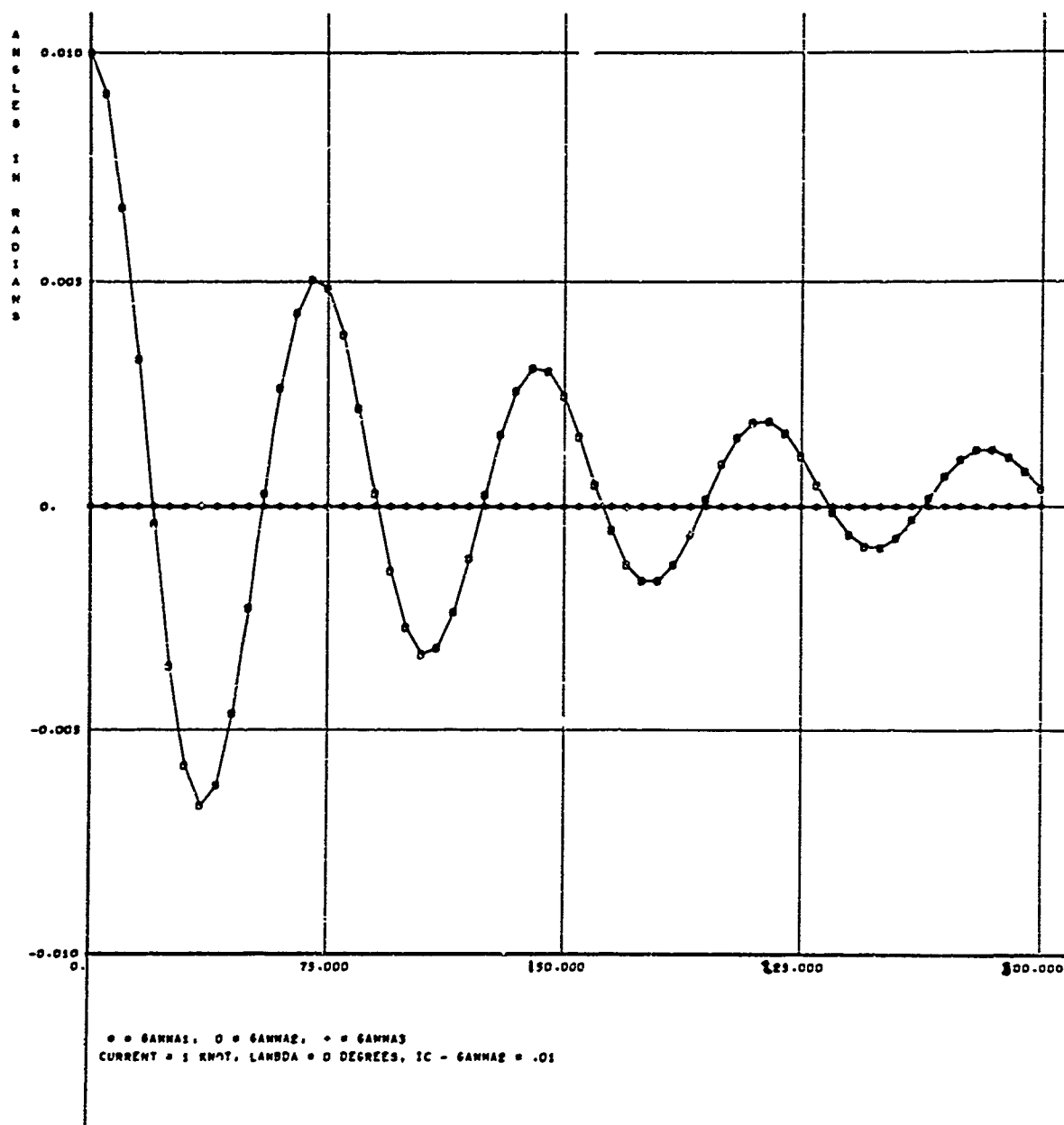Figure 36. Plots of Delta X, Delta Y, and Delta Z Against Time

52

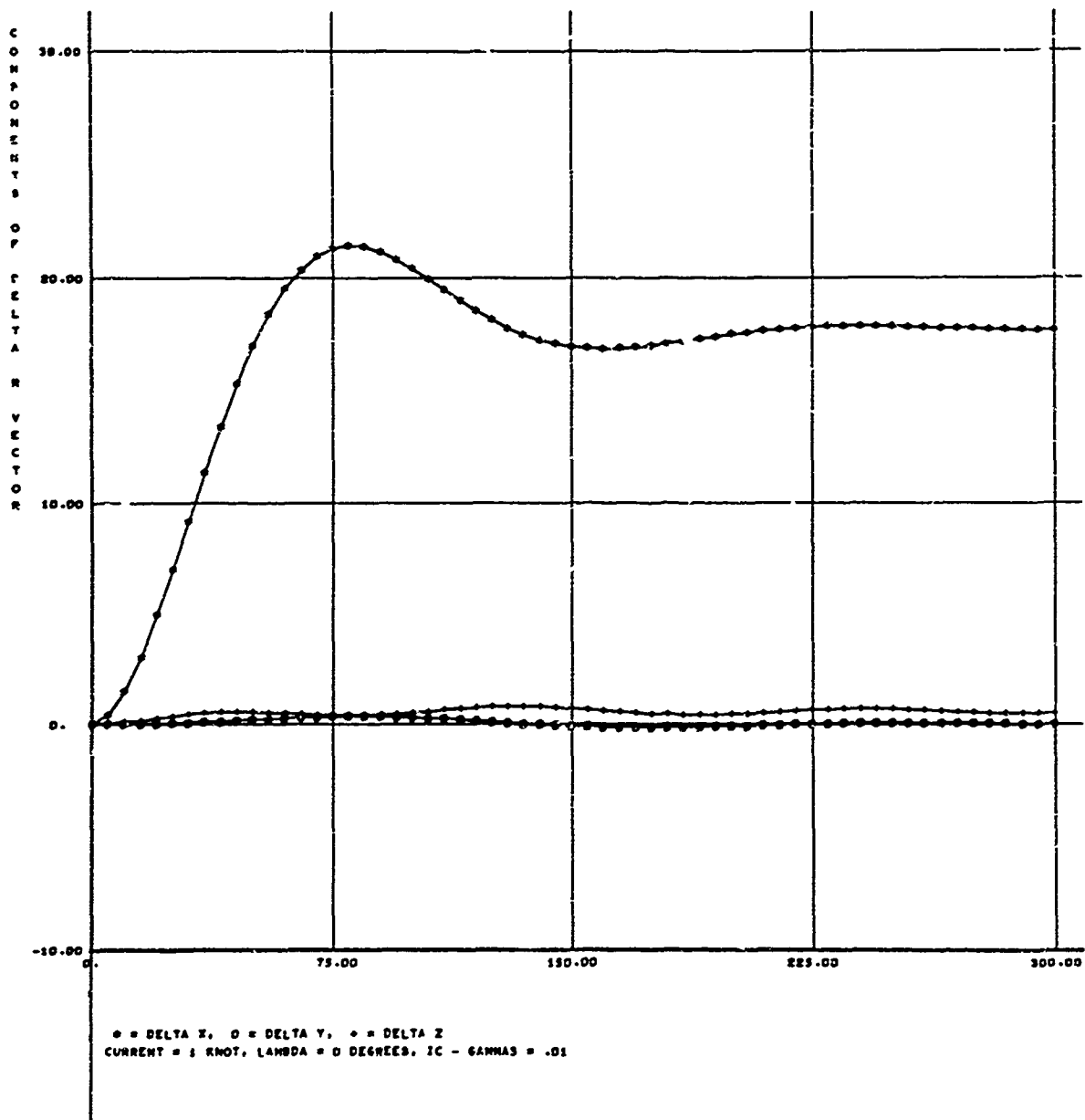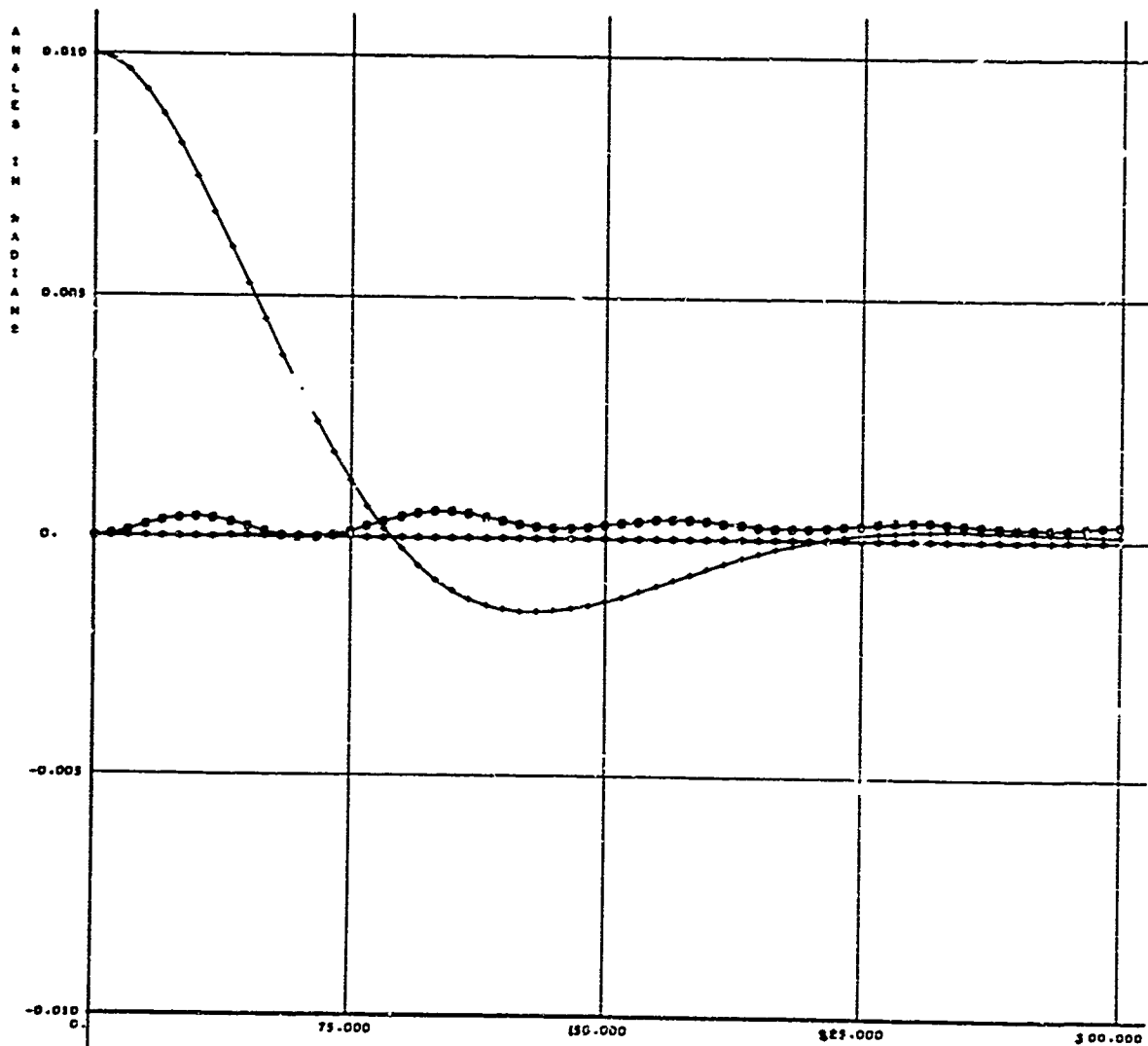Figure 37. Plots of Gamma 1, Gamma 2, and Gamma 3 Against Time

53

Figure 38. Plots of Delta X, Delta Y, and Delta Z Against Time

54

Figure 39. Plots of Gamma 1, Gamma 2, and Gamma 3 Against Time

The direct integration of the equations of motion was quite time consuming because of rapid attitude oscillations superimposed on the slow translational motion. It was found, however, that very accurate results could be obtained for the translational motion by taking the attitude angles identically equal to zero. That is, the small attitude motions usually encountered have a negligible effect on the translations and, thus, that part of the coupling could be ignored. Likewise, by assuming various fixed displacements of the mass center and integrating the attitude motion over several cycles one can get a rather good approximation of the attitude motions. In that manner, this part of the coupling was also alleviated.

Figures 40 through 43 show the translational motion resulting from digital simulations. Figure 40 shows the Δx motion caused by sudden application of a 1/4 knot current to a sphere in equilibrium. The slow response (with a period of about 1 hour!) reflects the extremely large mass involved. The displacement is a small fraction of the height above the ocean bottom. Figures 41 through 43 show the effects of a 1/2 knot current under the same initial conditions at angles of incidence $\lambda = 0, 12,$ and 24 degrees, respectively. The effects then repeat because of symmetry. We note the rather slow and underdamped behavior. The displacements are not, however, large. Possibly the number and/or size of the anchor cables can be reduced.

Figures 44 through 49 give results for the simulation of attitude motions. Figure 44 shows the effect of an initial displacement of 0.1 radian. Figures 45 through 48 show the attitude motions as excited by initial displacements of the mass center $\Delta x = 20, 40, 60, 80$ feet, respectively. Note the rapid convergence to a static reorientation and high-frequency oscillations. The steady-state angular displacement is no greater than 0.04 radian. Figure 49 shows the attitude motions for initial displacements $\Delta x = 60$ feet and $\Delta y = 20$ feet. This leads to angular displacements about both the x and y axes.

It seems that steady-state angular displacements are somewhat greater for the sphere than the tetrahedral structure, but still quite tolerable.
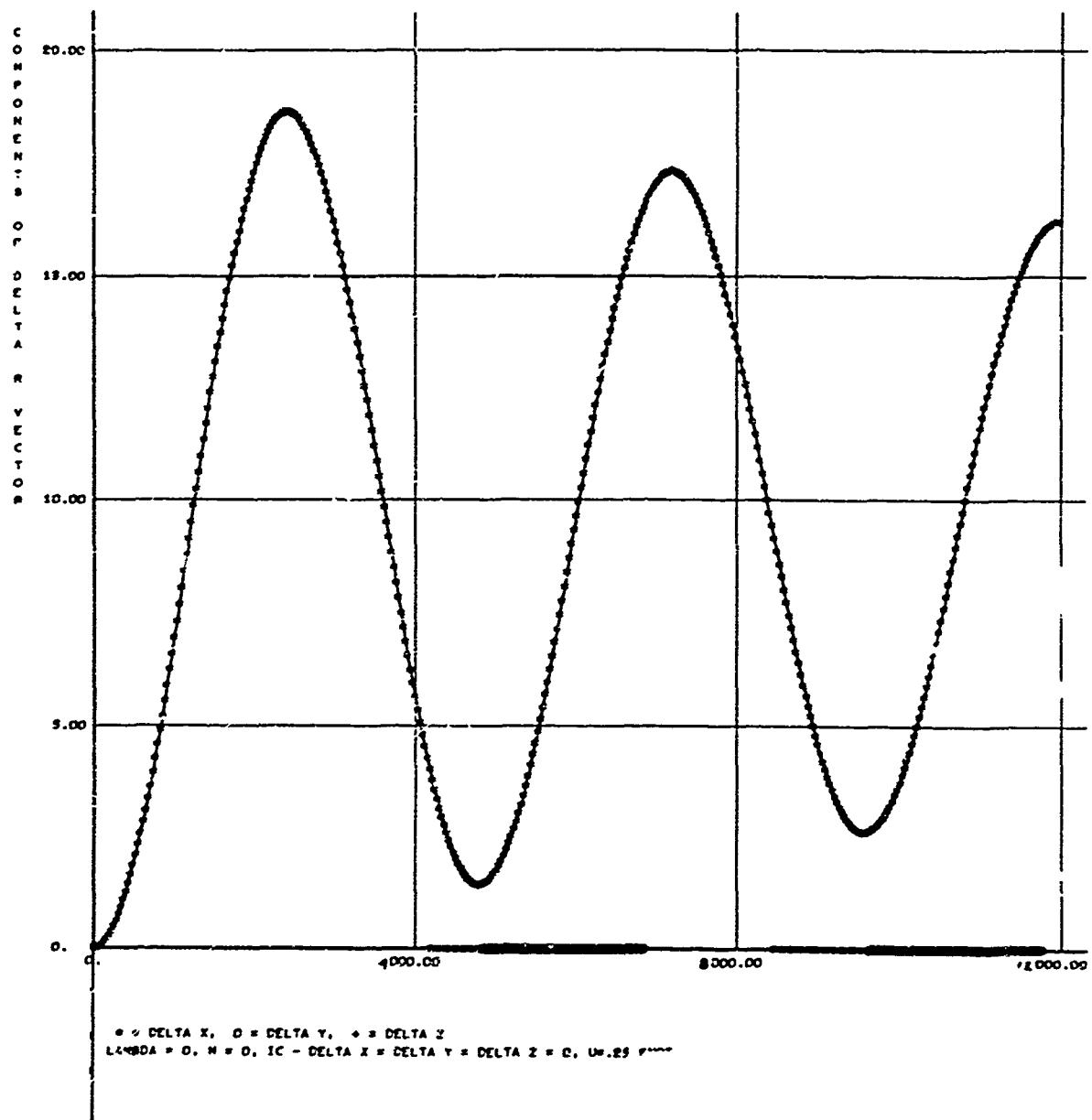
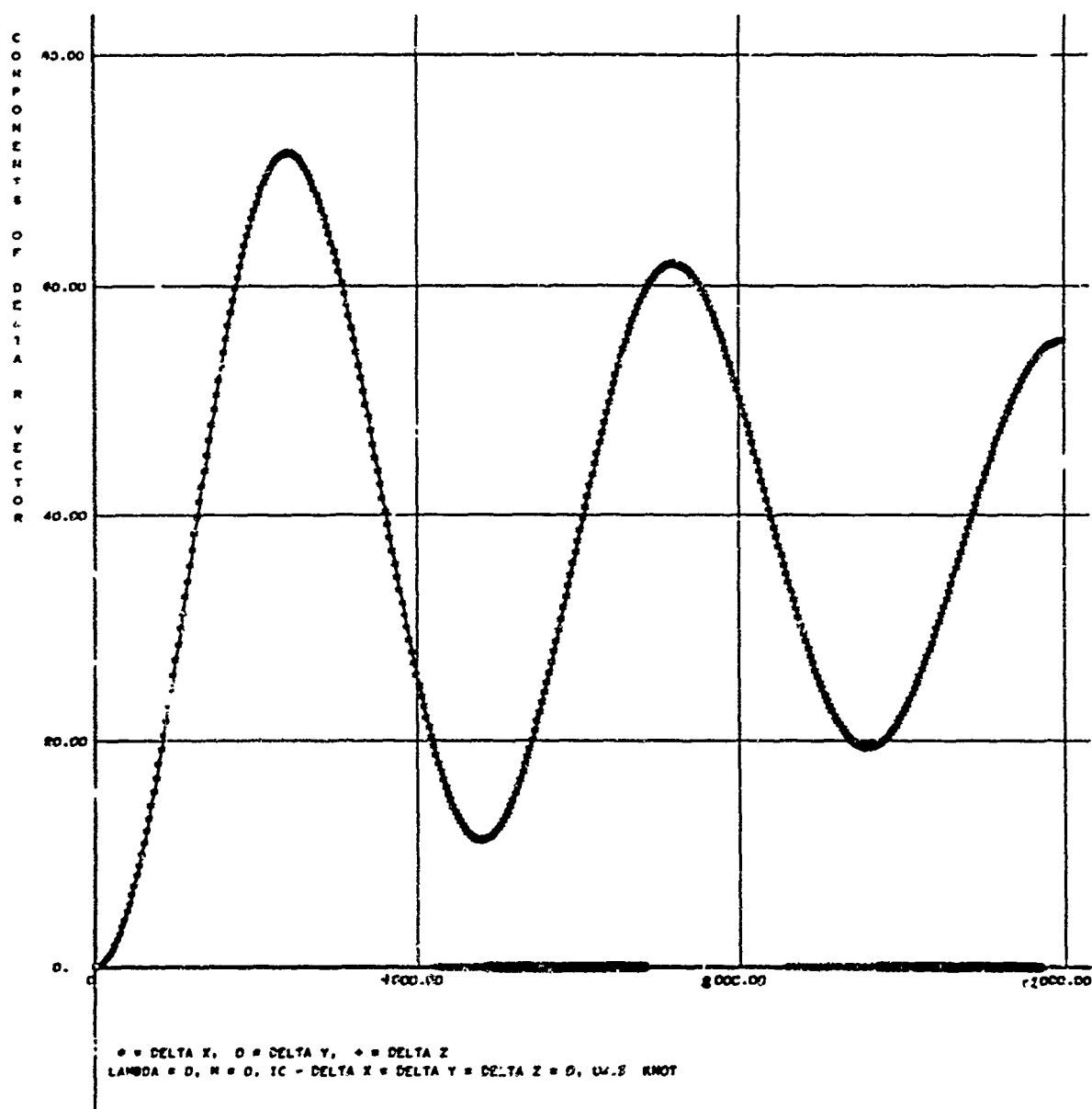Figure 40. Plots of Delta X, Delta Y, and Delta Z Against Time

57

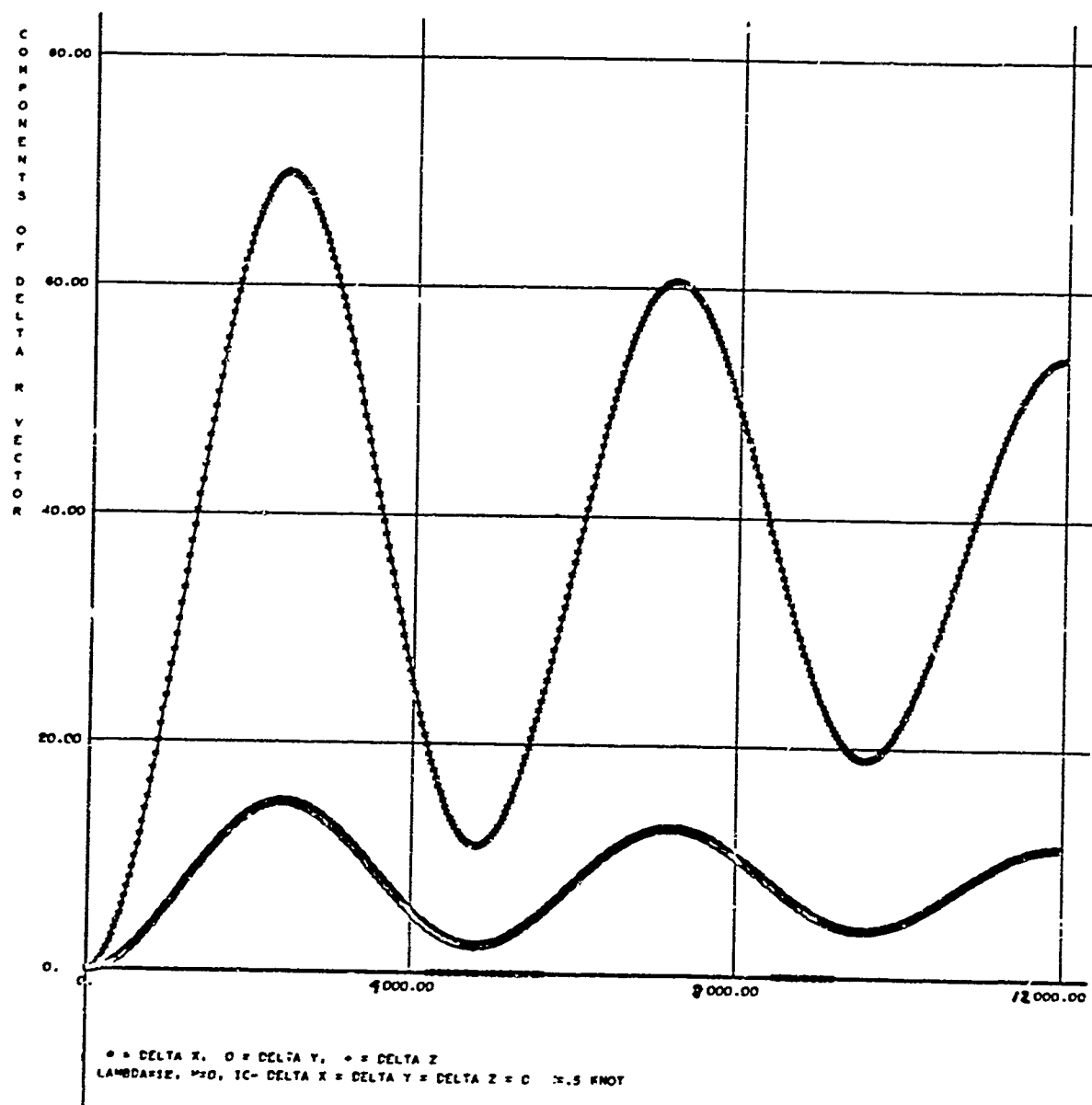Figure 41. Plots of Delta X, Delta Y, and Delta Z Against Time

58

Figure 42. Plots of Delta X, Delta Y, and Delta Z Against Time
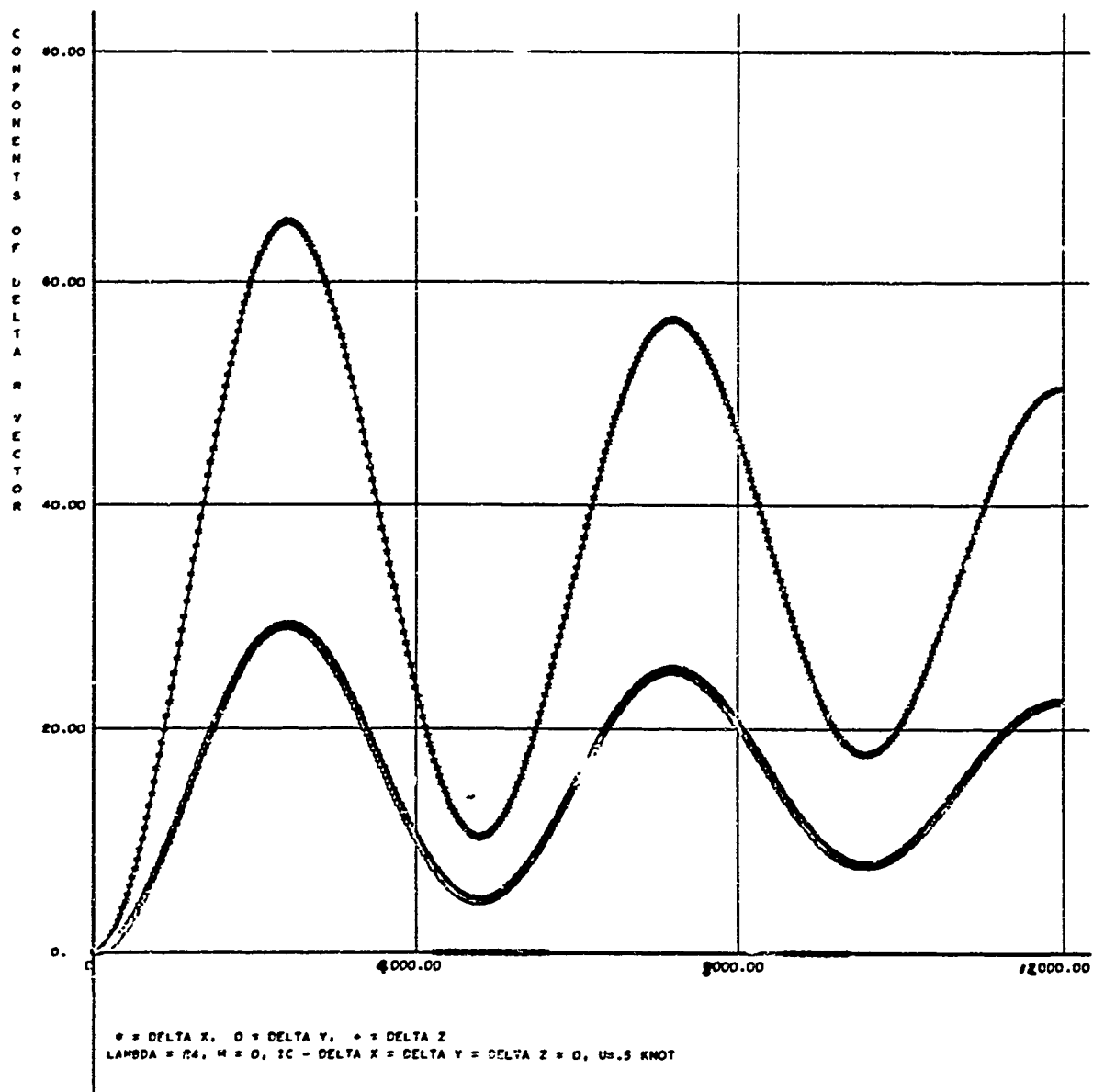
59

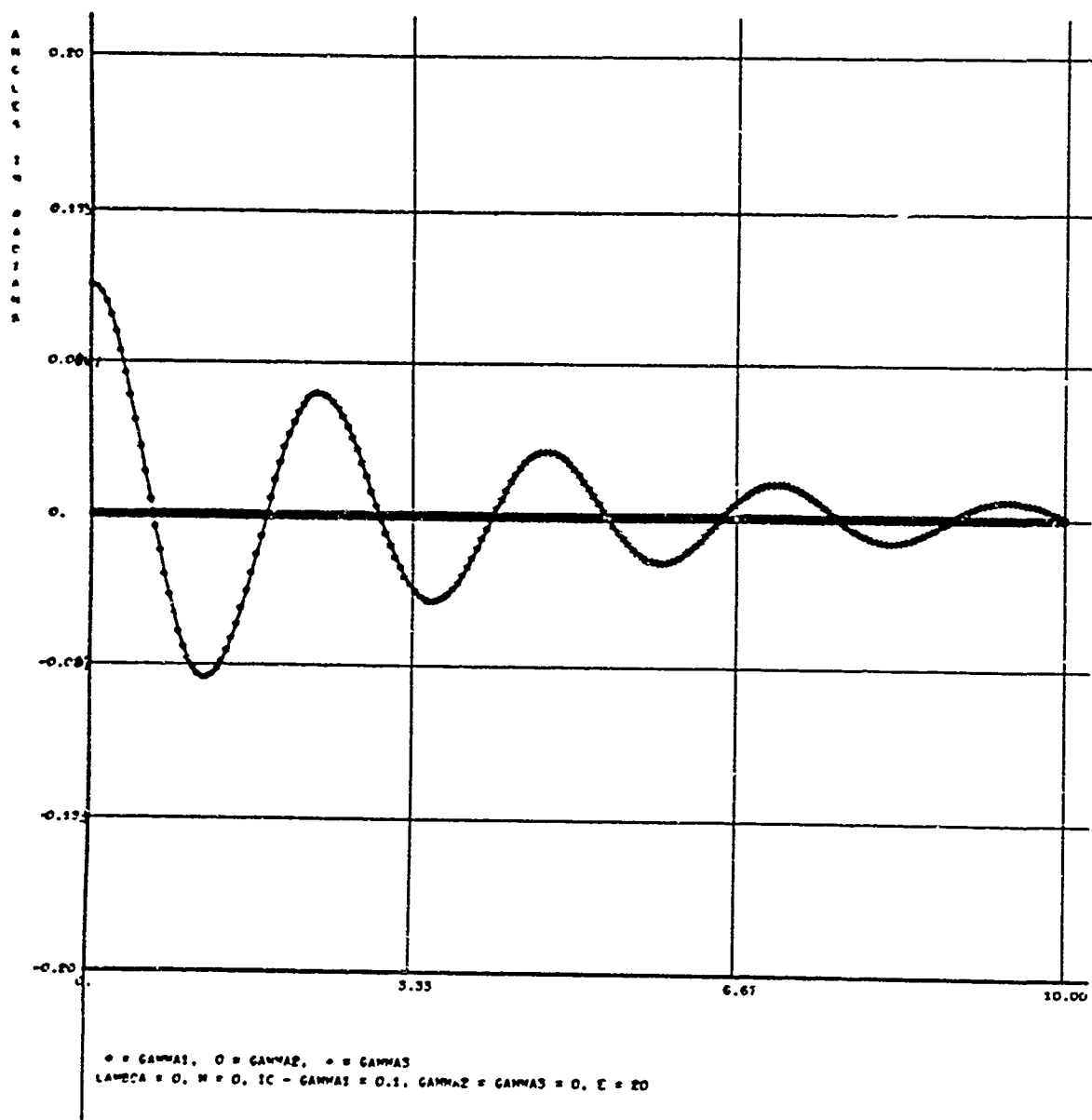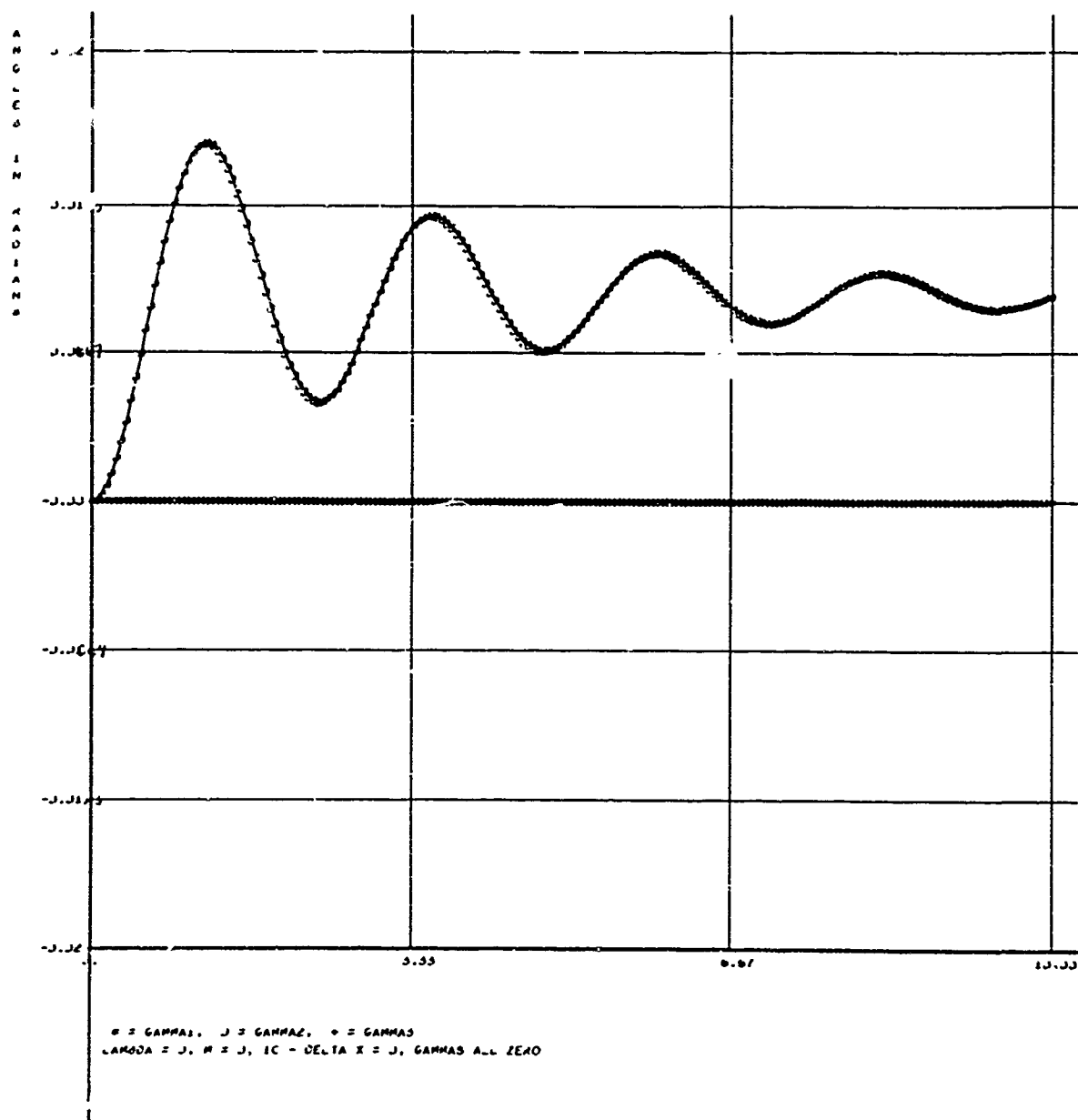Figure 43. Plots of Delta X, Delta Y, and Delta Z Against Time

60

Figure 44. Plots of Gamma 1, Gamma 2, and Gamma 3 Against Time

61

Figure 45. Plots of Gamma 1, Gamma 2, and Gamma 3 Against Time

Figure 46. Plots of Gamma 1, Gamma 2, and Gamma 3 Against Time

63

+ = GAMMA1,   O = GAMMA2,   + = GAMMA3
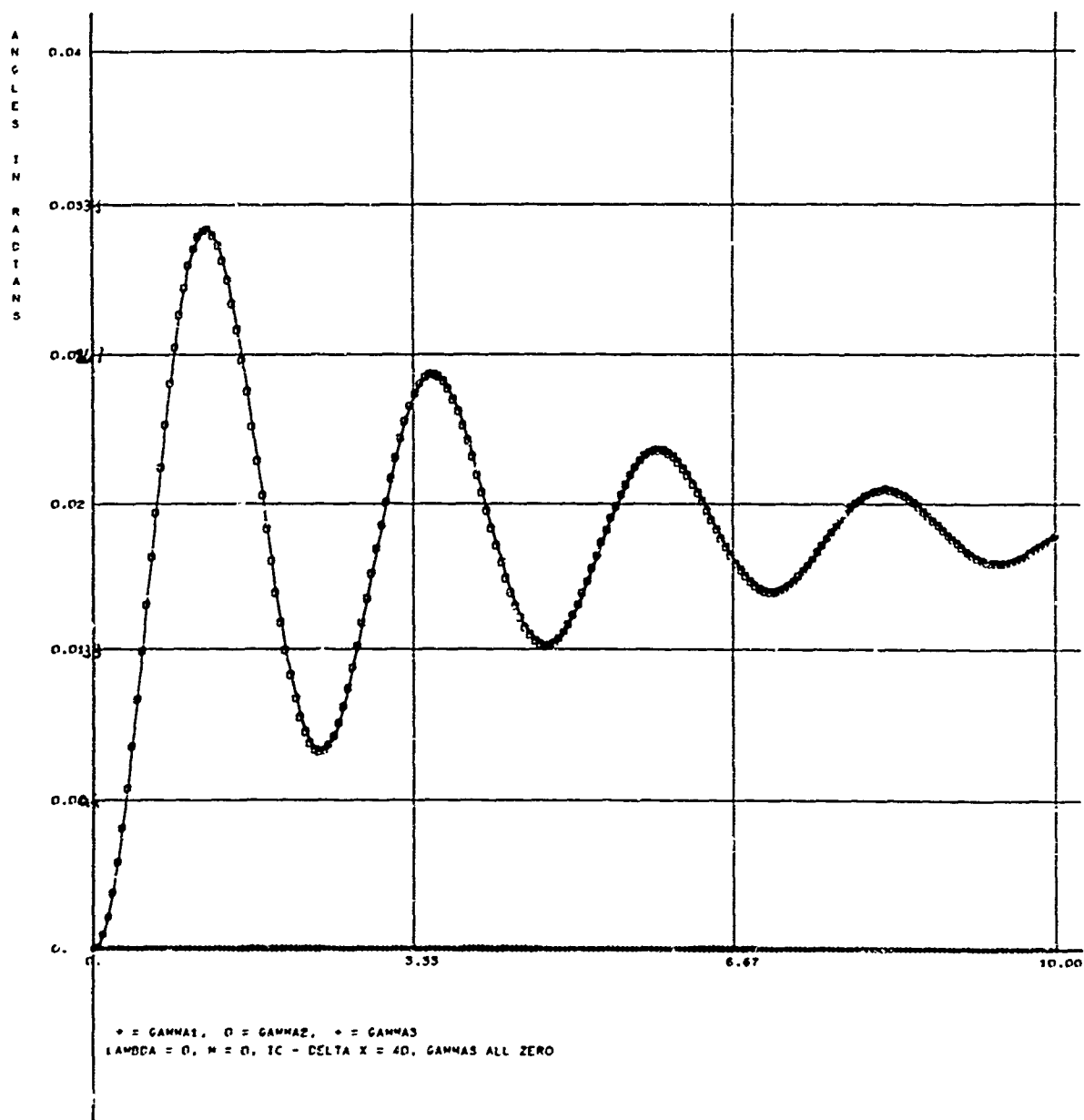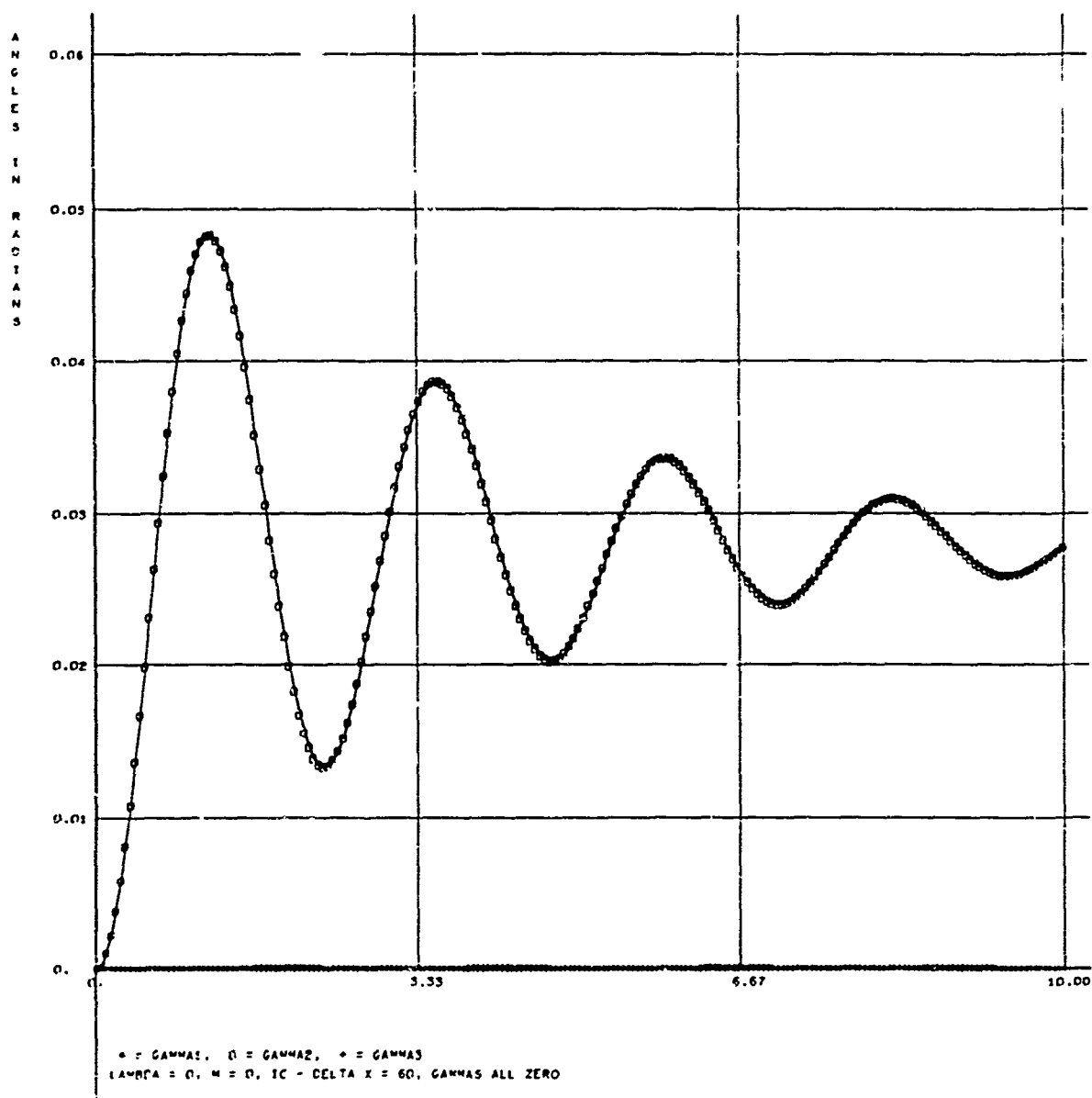LAMBDA = 0, M = 0, IC - DELTA X = 60, GAMMAS ALL ZERO

Figure 47. Plots of Gamma 1, Gamma 2, and Gamma 3 Against Time

Figure 48. Plots of Gamma 1, Gamma 2, and Gamma 3 Against Time

65

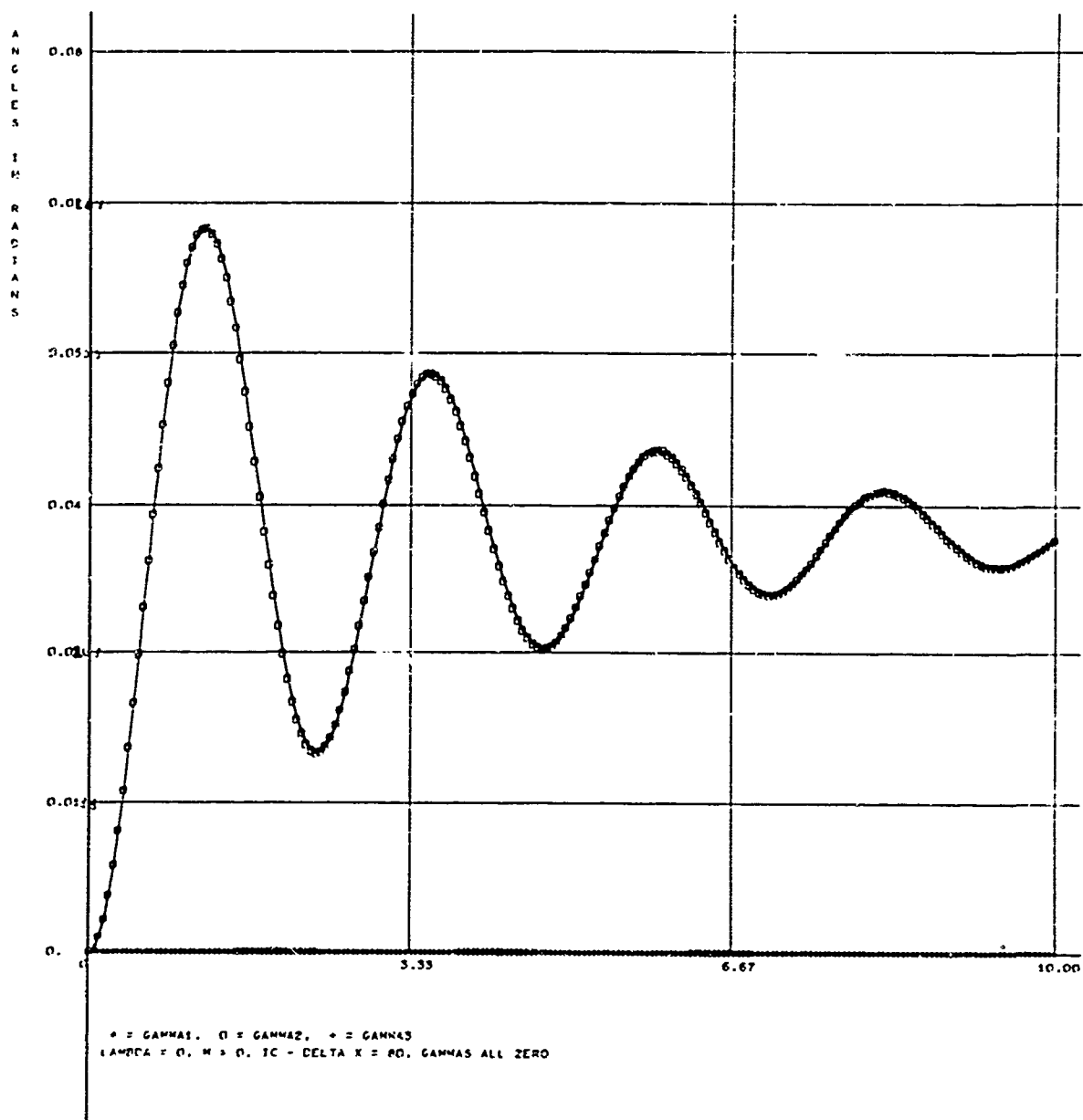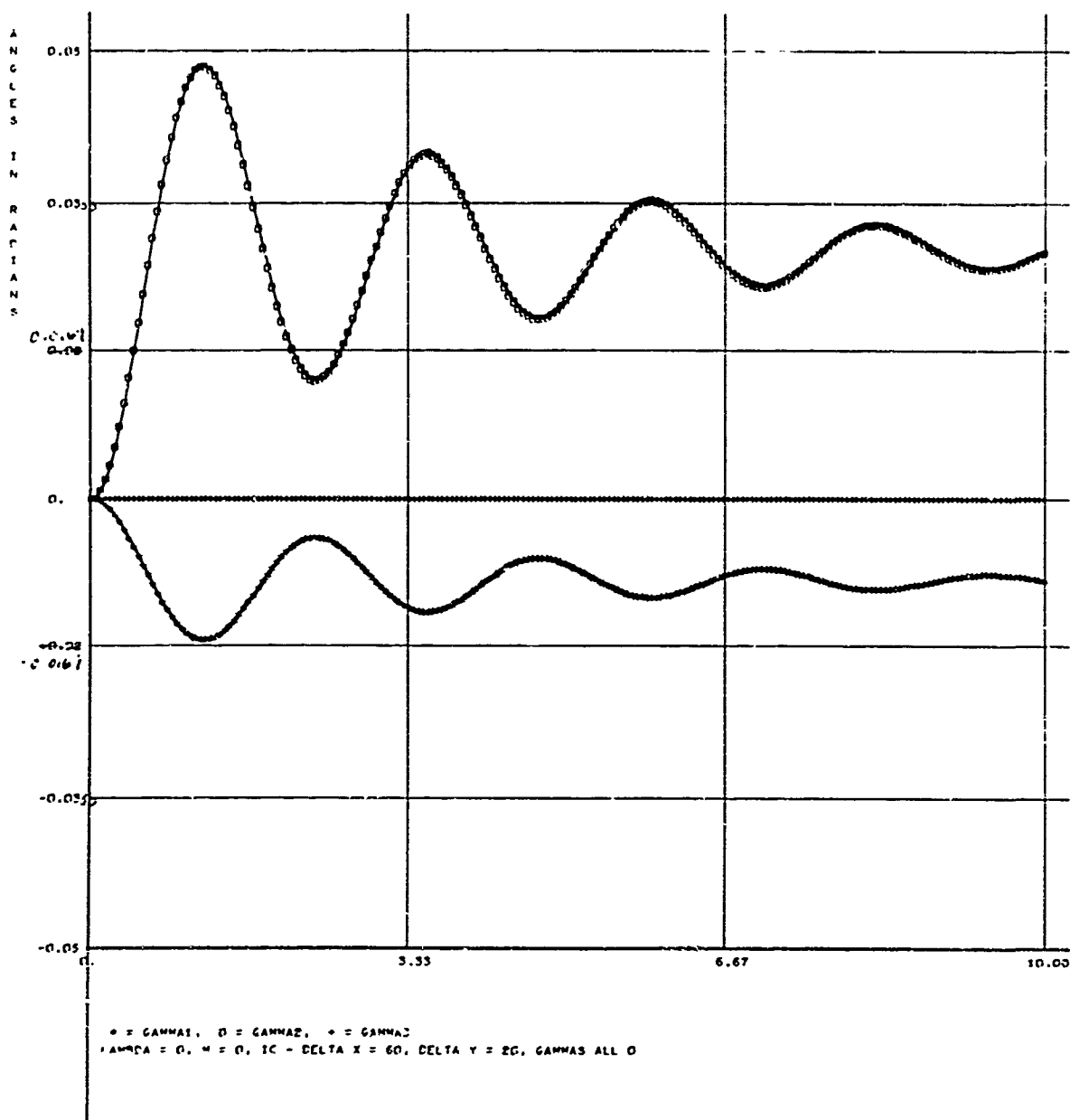Figure 49. Plots of Gamma 1, Gamma 2, and Gamma 3 Against Time

66

DOCUMENT CONTROL DATA · R & D

(Security classification of title, body of abstract and indexing annotation must be entered when the overall report is classified)

1. ORIGINATING ACTIVITY (Corporate author)	2a. REPORT SECURITY CLASSIFICATION
Bell Telephone Laboratories, Incorporated Whippany, New Jersey	Unclassified
	2b. GROUP

3. REPORT TITLE

The Analysis of Mooring Systems and Rigid Body Dynamics for Suspended Structures

4. DESCRIPTIVE NOTES (Type of report and inclusive dates)

Technical Report No. 14

5. AUTHOR(S) (First name, middle initial, last name)

J. M. Gormally and R. Pringle

6. REPORT DATE	7a. TOTAL NO. OF PAGES	7b. NO. OF REFS
December 30, 1966	72	6

8a. CONTRACT OR GRANT NO	9a. ORIGINATOR'S REPORT NUMBER(S)
N00014-66-C-0005	No. 14
b. PROJECT NO. RF 001-03-01	
c. 17x1319.1451	9b. OTHER REPORT NO(S) (Any other numbers that may be assigned this report)
d. 17501-14	

10. DISTRIBUTION STATEMENT

The distribution of this report is unlimited.

11. SUPPLEMENTARY NOTES	12. SPONSORING MILITARY ACTIVITY
	Office of Naval Research

13. ABSTRACT

In this report the response of a moored body to current loadings is investigated. A nonlinear analysis of the steady-state deflections of bipod and tripod moorings is made in Parts I and II. The mooring cables are assumed to be extensible and are loaded with constant gravity and current drag forces. It is shown that the cable weight-in-water is a significant factor in the deflection limited design of a cable system.

In Part III the cable mooring system is represented by linearized equations. Numerical integration is used to investigate the transient rotational and translational response of the moored body to changes in the ambient current.

DD FORM 1473
1 NOV 65

14 KEY WORDS	LINK A		LINK B		LINK C	
	ROLE	WT	ROLE	WT	ROLE	WT
Suspended Structures						
Deflections						
Buoyed Bipod Systems						
Buoyed Tripod Systems						
Mooring Systems						